

# Liquid Crystal Electropolymerisation Under Magnetic Field and Resultant Linear Polarised Electrochromism

Hiromasa Goto,<sup>1,\*</sup> Shigeki Nimori<sup>2</sup>

<sup>1</sup>Graduate School of Pure and Applied Sciences, Institute of Materials Science,  
University of Tsukuba, Tsukuba, Ibaraki 305-8573, Japan

<sup>2</sup>National Institute for Materials Science (NIMS), Tsukuba Magnet Laboratory, Sakura,  
Tsukuba 3-13, Japan

\*Correspondence to H. Goto

Tel: +81-298-53-5128, fax: +81-298-53-4490

Email: [gotoh@ims.tsukuba.ac.jp](mailto:gotoh@ims.tsukuba.ac.jp)

## **Abstract**

The electrochemical preparation of poly(3,4-ethylenedioxythiophene) (PEDOT) is conducted in liquid crystal (LC) electrolyte solution with nematic (N), cholesteric (Ch\*), and smectic A (SmA) phases under a magnetic field. The polymer imprints the molecular arrangement of the LC electrolyte during the polymerisation process. The oriented polymers thus obtained displays optical texture characteristics that resemble those of the LC electrolyte solution. Especially, visualization of SmA domain through PEDOT fibrils is achieved. The magnetic alignment produces linear optical polarisation for the polymers. The PEDOTs thus prepared exhibit good reproducible electroactivity. The present electropolymerisation under magnetic field affords polymer films with linear polarised electrochromism.

## **Introduction**

Top-down and bottom-up methods are considered for the manipulation of molecular ordering and processing. Top-down methods have commonly been employed, such as etching and photolithography, which require externally controlled and highly technical micro-processing methods. However, bottom-up approaches such as chemical molecular

self-assembly or molecular recognition have the advantage of simplicity if a suitable method can be established.<sup>[1,2]</sup> Bottom-up technologies that employ strongly ordered aggregation are another promising approach.<sup>[3]</sup>

The application of an oriented magnetic field can yield highly oriented functional materials. Organic compounds containing phenylene groups have anisotropy with diamagnetic susceptibility. This property is subject to magnetic orientation, which results in morphological changes under a magnetic field.<sup>[4]</sup> The magnetic orientation of poly(ethylene terephthalate)<sup>[5]</sup> and carbon nanotubes<sup>[6]</sup> has been successfully carried out. In addition, magnetic tuning of electrochemical reactivity through controlled surface orientation of catalytic nanowires has been studied.<sup>[7]</sup> Electropolymerisation in isotropic acetonitrile solution under a magnetic field has also been reported.<sup>[8]</sup>

Liquid crystal (LC) materials are promising candidates for the preparation of ordered polymers. LCs have good response to external force fields, such as magnetic fields, due to their fluidity and diamagnetic anisotropy.<sup>[9]</sup> In previous research, the magnetic orientation of liquid crystalline  $\pi$ -conjugated polymers was performed at high temperature ( $>100$  °C).<sup>[10]</sup> However, the magnetic orientation of polymer LCs requires a considerable amount of time, due to their high viscosity and their need to be maintained at the polymer LC temperature range during the orientation process in a magnetic

chamber. Furthermore, the oriented polymers exhibit no electrochemical doping-dedoping driven electrochromism.

LC phases are determined by their molecular arrangement. LC materials exhibit nematic (N), cholesteric (Ch\*), and smectic (Sm) phases. The primary feature of molecular organisation in nematic liquid crystal (NLC) is the orientational ordering of the molecular axis along a particular direction, where the average direction of the long axis defines the director ( $n$ ), which may be treated as a vector.<sup>[11]</sup> NLCs have the least ordering and highest symmetry of the LC phases (Fig. 1(a)). The schlieren texture, which can be observed using a polarised optical microscope (POM), appears as a brush-like pattern that reflects the disclinations and directors of individual LC molecules in the system. Cholesteric liquid crystals (Ch\*LC) is a chiral form of NLC, and has a spontaneous one-handed macroscopic helical structure with a twist axis perpendicular to the local director, as shown in Fig. 1(b). The molecules of smectic A (SmA) are parallel to each other and are arranged in layers with the long axis perpendicular to the layer plane, as shown in Fig. 1(c).

Fig. 1

The surface structures of polymers synthesised in LC matrices using light-induced polymerisation methods have been studied.<sup>[12-16]</sup> A LC solvent was employed for the

preparation of polyacetylenes using the Ziegler–Natta catalytic system over 20 years ago.<sup>[17–19]</sup> Syntheses of polyacetylene in NLC under an applied magnetic field<sup>[20]</sup> and using a gravity flow technique<sup>[21]</sup> were performed to obtain films with conductivity anisotropy. Furthermore, the preparation of polyacetylene films with Ch\*LC has been reported.<sup>[22]</sup> Although the polymers were obtained in the form of thin solid films, the formation of good ohmic contacts with electrodes for the preparation of electronic devices is difficult.

The functionalities of  $\pi$ -conjugated polymers, such as semiconductivity, light emission, and magnetic properties, can be enhanced by molecular arrangement. To obtain  $\pi$ -conjugated polymers with characteristic surface morphology, electropolymerisations in Ch\*LC<sup>[23]</sup> and lyotropic LCs (LC ordering is induced by the addition of solvents)<sup>[24–27]</sup> have been performed.

Poly(3,4-ethylenedioxythiophene) (PEDOT) and its derivatives are the most promising polymers in the plastic electronics research field, because PEDOT exhibits good electroactivity and durability. Synthesis of 2,3,2',3',2'',3'-hexahydro-[5,5':7',5'']*ter*[thieno[3,4-b]-[1,4]dioxine] (*ter*EDOT) with high resolution electronic spectra and good electrochromic properties has been reported.<sup>[28,29]</sup> Recently, the preparation of *ter*EDOT by a convenient method and

subsequent polymerisation to afford PEDOT with fibril structure was developed.<sup>[30]</sup> We have investigated electro-preparative methods to obtain chiroptical electroactive polymers using low-molecular-weight Ch\*LC electrolyte solutions. We developed a sandwich cell electrochemical polymerisation method,<sup>[31,32]</sup> which is valid for electropolymerisation in LC electrolyte solution.

In this study, we performed the polymerisation of *ter*EDOT in N, Ch\*, and SmA electrolyte solutions under a magnetic field for the preparation of PEDOT with visible LC-like oriented morphology and optical anisotropy. The polymer realises the LC structure through transcription of the molecular arrangement of the LC matrix. The electro-prepared samples have good adhesion to indium tin oxide (ITO)-covered glass electrodes, providing good ohmic contact; the electronic contact allows electrochemical charge injection and discharge of the polymer. The polymers thus obtained also exhibit linear optical polarisation. A combination of the bottom-up technique with LC and magnetic processing methods has realised oriented electroactive polymers. The polarisation properties and electrochromism of PEDOT affords linear polarised electrochromism.

## **Experiment**

## LC electrolyte preparation

LC electrolytes were prepared for electrochemical polymerisation in NLC, Ch\*LC, and SmALC. Firstly, NLC electrolyte solution was prepared with 4-cyano-4'-hexyl biphenyl (6CB). 6CB, which has a thermotropic LC character, can be regarded as a solvent for fluidity. The addition of a supporting salt to 6CB imparts ionic conductivity. Therefore, a mixture of LC and a supporting salt can be used as an electrolyte solution for electrochemical polymerisation, instead of conventional systems such as tetrabutylammonium perchlorate (TBAP) or lithium perchlorate in acetonitrile.

The addition of a small amount of an optically active molecule as a chiral inducer to Ch\*LC can induce the formation of Ch\*LC with helical structures on a mesoscopic level.<sup>[33,34]</sup> Ch\*LC electrolyte solution was prepared by the addition of cholesteryl pelargonate as a chiral inducer and TBAP (supporting salt), and then *ter*EDOT (monomer) to 6CB. The electrolyte exhibits a Ch\* phase LC at room temperature.

SmALC generally has a higher LC temperature range and higher viscosity than that of NLC, because SmALC has a highly ordered (layered) structure. The high viscosity results in low mobility of the monomers and ions in the SmA matrix, and the depression of polymerisation activity in the LC solution. Therefore, a mixed LC system was employed as the electrolyte solution to compensate for these drawbacks, because a

mixed LC system has decreased viscosity and a lower LC temperature range.

A mixture ratio of 1/2 = 6CB/8OCB (w/w) exhibits the SmA phase at room temperature with moderate to low viscosity. The preparation of LC electrolyte solution was carried out in an argon atmosphere, because *ter*EDOT has quite high polymerisation activity. In addition, the LC electrolyte solution was handled carefully when heating during the experiment to avoid thermally induced polymerisation. The constituents of the LC electrolyte solutions employed in this study are summarised in Scheme 1. Details for the preparation of the LC electrolytes are described in the Experimental section of the Supplementary Information.

Scheme 1.

Fig. 1.

## Polymerisation

LCs were employed as electrolyte solutions for electrolytic polymerisation in place of conventional systems that consist of a supporting salt in isotropic solution. The polymerisations were carried out using the sandwich cell polymerisation method,<sup>[30,31]</sup> which enables electropolymerisation to occur in a small space within a magnetic



chamber.

Prior to polymerisation, the electrolyte solution was heated in a vial to approximately 60 °C under an argon atmosphere, in order to completely dissolve the mixture in the 6CB LC solvent. Setting up for electropolymerisation was then carried out by injecting the LC mixture (NLC, SmALC, or Ch\*LC) between sandwiched ITO-coated glass electrodes ( $9 \Omega/\text{cm}^2$ ) with a Teflon sheet (ca. 0.2 mm thick) as a spacer (Fig. 1(d)). The use of two electrodes separated by a narrow gap compensates for the IR drop (ohmic overpotential) of the low ionic conductivity LC electrolyte. The reaction cell was quickly placed in a drum type magnetic chamber at 25 °C. Subsequently, the magnetic field was gradually increased (0.3 T/min) up to the appropriate strength and the cell was left for 30 min in the magnetic field. A voltage of 4.0 V was then applied across the cell to induce potentiostatic electrolytic polymerisation under the magnetic field. After 30 min, the cell was quickly removed from the magnetic chamber, and the plastic clip holding the sandwiched polymerisation cell together was detached (Fig. 1(e)). The insoluble and infusible PEDOT thin film coating the anode side of the ITO electrode was then washed with methanol, water, acetonitrile, and acetone. The molecular structures, abbreviations of the polymers, and reaction conditions used for the electropolymerisations under magnetic field are

summarised in Scheme 1. Furthermore, electrochemical polymerisations of *ter*EDOT under zero magnetic field were carried out in N, Ch\*, and SmA at room temperature (LC state). Polymerisations in SmA at 80 °C (isotropic state) and in 0.1 M acetonitrile solution (standard method) were also conducted to yield PEDOT-ACN and PEDOT-SmA<sub>0T</sub>iso (Scheme 1).

## Results and discussion

### Optical texture

A LC-free polymer synthesised in nematic electrolyte solution under zero magnetic field (PEDOT-N<sub>0T</sub>) exhibited a schlieren texture consisting of microfibrils with twofold brushes under cross-polariser conditions of the POM. Fig. 2(a) shows a POM image obtained by insertion of a gypsum first-order red plate. The direction of insertion of the red plate (from upper left to lower right) colours the polymer surface red, and then blue in the opposite direction (from upper left to lower right). This uniaxial optical property has the same character as NLCs, which suggests that a molecular level transcription of the NLC ordering of PEDOT occurred during electropolymerisation. The polymer prepared under 4 T (PEDOT-N<sub>4T</sub>) has an oriented schlieren texture with microfibril structure (Fig. 2(b)), although the polymer exhibits no macroscopic domain structure,

because NLC forms no LC domain. The fibrils are across and between the stretched schlieren disclination lines. The insolubility of the polymer in the LC electrolyte solution during the polymerisation process facilitates phase separation to produce the pure polymer with LC ordering.

Fig. 2.

The polymerisation product of *ter*EDOT in Ch\*LC electrolyte solution under zero magnetic field (PEDOT-Ch\*<sub>0T</sub>) exhibited a vortex structure under the POM.<sup>[30]</sup> The optical texture is derived from macroscopic director ordering of the Ch\*LC electrolyte solution with the molecular transcription mechanism.

The vortex structure undergoes elongation along the direction of magnetic field (2 T) and forms a vortex ellipsoid, as shown in Fig. S1 (Supplementary information). The increase in the magnitude of the magnetic force stretches the vortex texture to produce texture lines. Under a magnetic field of 4 T, the stripes of the polymer grow to linear zebra-like stripes along the magnetic field (Fig. 2(c)). The stripes are derived from the helical periodic structure, which indicates that the helical axis is oriented in the direction perpendicular to the magnetic field. The templated polymer (PEDOT-Ch\*<sub>4T</sub>) exhibits visually confirmable polarisation, as shown in Fig. S2, Supplementary information.

Application of 9 T resulted in partial unwinding of the helical structure of Ch\*LC. Furthermore, the Lorentz force operates in the horizontal direction perpendicular to the magnetic force and the applied electric field during polymerisation, which results in disordering of the LC alignment and unsatisfactory polymer orientation. Therefore, a magnetic field of 4 T is a more favourable magnitude to yield oriented products by the present polymerisation.

SmA has a layered structure with higher ordering than NLC and Ch\*LC. The SmA phase exhibits a focal conic fan-shaped and polygonal textures under appropriate anchoring conditions to the substrate (Fig. S3(a), Supplementary information). The SmALC electrolyte solution containing monomer has a stable SmA phase at room temperature, and magnetic orientation affords oriented domains along the magnetic field, as shown in Fig. S3(b), Supplementary Information. Fig. 3(a,b) and Figs. S4, S5 (Supplementary Information) show POM images of PEDOT prepared in SmALC electrolyte solution under zero magnetic field (PEDOT-SmA<sub>0T</sub>). These structure is very similar to that of smectic A liquid crystals. Scanning electron microscopy (SEM) images show the PEDOT-SmA<sub>0T</sub> domain structure. Cocoon-like (Fig. 3(c)) and fan-shaped structures (Fig. 3(d)) of the PEDOT derived from polygonal textures and focal conic fan-shaped textures of SmALC were observed. The polygonal texture (Figs.

3(a) and S5, Supplementary information) is very similar to that of a previously reported SmALC material for 2-[4-*n*-pentyl-phenyl]-5-[4-*n*-pentyloxy-phenyl]-pyrimidine.<sup>[34]</sup> It is noteworthy that the LC domain consists of fibril structures, and the fibrils are arranged in the vertical direction to the lateral direction of individual domains. This could be due to the fact that the fibrils grow along the layer boundary of the SmA phase. The distance between fibrils is related to the layer distance of SmA. The blue and red colour distribution in the POM image with insertion of gypsum first-order red plate demonstrates optically uniaxial materials, which is characteristic of SmA, as shown in Fig. 3(b) and Fig. S5. These results suggest that the PEDOT is imprinted with the SmA molecular arrangement and birefringence, although the PEDOT has no LC property (fluidity). Fig. 3(e) taken from a direction oriented 35 ° from the surface demonstrated that the head parts of the domains form multiple circles. This image also indicates that the characteristic surface derived from SmA ellipsoidal structure. This method allows visualization of SmA domain through PEDOT. Furthermore, the polymer exhibits beautiful Morpho butterfly-like sky-blue iridescence, due to the periodic arrangement of fibrils derived from the distance between layers in the domain, which behave as a diffraction grating to display structural colour (Fig. S6 (inset), Supplementary Information). Laser irradiation (532 nm) of the sample shows an aligned diffraction

pattern (Fig. S6, Supplementary Information).

A polymer prepared from *ter*EDOT in SmA at 80 °C (isotropic state) displays small fibril structures without a fan-shaped structure, and PEDOT prepared in isotropic acetonitrile solution (standard method) shows no clear fibril structures, which suggests that the molecular arrangement of the LC functions to produce the macroscopic order of the resultant polymers.

Magnetic orientation under 4 T causes macroscopic arrangement of the LC domains. The individual fan-shaped domains align along the magnetic field. The fibrils arrange perpendicular to the domain alignment and direction of the magnetic field, as shown in the POM image of Fig. 4(a). The SEM images in Fig. 4(b) and magnification image of Fig. 4(c) confirm that the PEDOT clearly forms fibril structures and is aligned perpendicular to the direction of the magnetic field. Note that the polymer prepared in SmA under magnetic field (4T) partly shows an aloe-leaf-like structure, as shown in Fig. S7 (Supplementary Information).

Fig. 3.

Fig. 4.

## IR

IR spectra of the polymers prepared in acetonitrile solution, NLC, Ch\*LC, and SmALC at room temperature (LC state), and SmA at 80 °C are shown in Fig. S8 (Supplementary Information). The PEDOT displays no absorption bands related to the characteristic absorption bands of 6CB ( $2227\text{ cm}^{-1}$ ,  $\nu_{\text{CN}}$ , terminal CN group) or cholesteryl pelargonate ( $1737\text{ cm}^{-1}$ ,  $\nu_{\text{C=O}}$ , ester moiety). The IR spectra confirm that although these polymers display different morphologies, they have the same chemical structure.

## CV

Cyclic voltammetry (CV) measurements of the PEDOT films (vs.  $\text{Ag}/\text{Ag}^+$ ) were performed in monomer-free 0.1 M TBAP/acetonitrile solution. During the oxidation (doping) process, an oxidation signal at  $-0.08\text{ V}$  (scan rate:  $100\text{ mV/s}$ ) was observed for PEDOT-SmA<sub>4T</sub>, while reduction signals were observed at  $-0.51\text{ V}$  (scan rate:  $100\text{ mV/s}$ ) (Fig. S9, Supplementary Information). CV results for PEDOT-ACN (the PEDOT was prepared by 10 times repeating scan between  $-0.8\text{ V}$  and  $1\text{ V}$  in 0.1 M acetonitrile, [monomer] = 0.01 M, scan rate =  $50\text{ mV/s}$ ) at room temperature and PEDOT-SmA<sub>0T</sub>iso were shown in Fig. S10. Although the polymers display oxidation signals at slightly

high potentials and reduction signals at low potentials, the polymers exhibit the same tendency as that of PEDOT-SmA<sub>4T</sub> (PEDOT-ACN: oxidation signal = -0.05 V, reduction signal = -0.56 V, 100mV/s; PEDOT-SmA<sub>0Tiso</sub>: oxidation signal = -0.05 V, reduction signal = -0.55 V, 100 mV/s).

Redox switching in monomer-free electrolyte solution indicates a well-defined and quasi-reversible redox process. The polymers prepared in NLC and CLC displayed the same tendency.

#### Optical absorption and linear polarised electrochromism

Fig. 5(a) shows *in situ* optical absorption spectra for the PEDOT film at various voltages in monomer-free 0.1 M TBAP/acetonitrile solution. The measurement cell included platinum wire as the counter electrode, an Ag/Ag<sup>+</sup> reference electrode, and PEDOT deposited on ITO. Application of a voltage in the monomer-free acetonitrile solution causes the oxidation of PEDOT, accompanied by a weakening of the  $\pi$ - $\pi^*$  transition of the main chain (600 nm). The colour of the PEDOT film also changes from purple to sky blue upon doping (oxidation), which is reflected by the emergence of a broad absorption band in the near IR (NIR) region due to electrochemical doping (Fig. 5(a), inset). The colour of the PEDOT film changed reversibly upon cycling of the



electrochemical doping/dedoping (oxidation/reduction) process. This redox behaviour is typical for electroactive conducting polymers. Polarised spectro-electrochemical results for PEDOT prepared by electropolymerisation in NLC and Ch\*LC under 4 T shows the same tendency as PEDOT-SmA<sub>4T</sub> (Figs. S11 and S12, Supplementary Information). Absorption maxima in the direction parallel to the polariser ( $Ab_{s//}$ ) for PEDOT-Ch\*<sub>4T</sub> and PEDOT-SmA<sub>4T</sub> were at longer wavelengths than those of the perpendicular direction ( $Ab_{s\perp}$ ), which suggests that the visual colour of the oriented sample is dependent on the direction of polarisation. Furthermore, the dichroic ratios of PEDOT-SmA<sub>4T</sub> at various potentials were higher than those of PEDOT-N<sub>4T</sub> and PEDOT-Ch\*<sub>4T</sub>. The wavelength of the  $\pi$ - $\pi^*$  transition of the main chain increases with ordering of the LC electrolyte solution [NLC < Ch\*LC < SmA; PEDOT-N<sub>4T</sub> (580 nm), PEDOT-Ch\*<sub>4T</sub> (596 nm), PEDOT-SmA<sub>4T</sub> (620 nm) (dedoped)]. PEDOT-ACN and PEDOT-SmA<sub>0Tiso</sub> display  $\lambda_{max}$  at around 500 nm, which is ascribed to the  $\pi$ - $\pi^*$  transition of the main chain, as shown in Figs. S13, S14 (Supplementary Information). The polymers displays good electrochromic properties; Fig. S14 (inset, Supplementary Information) shows the reversible change in absorption intensity at 500 nm ( $\pi$ - $\pi^*$  transition of main chain) and at 900 nm (polaron band). PEDOT-SmA<sub>4T</sub> displays the absorption peak at long wavelengths (80–120 nm red shift). These results indicate that

the LC state of the reaction field produces aggregation of the main chains, which results in improvement of the co-planarity of the main chains.

Polarised optical measurements of the aligned polymer were performed, in order to comprehend the orientational behaviour of the PEDOT polymer. Fig. 5(b,c) shows polarised spectro-electrochemical analysis results for PEDOT prepared by electropolymerisation under 4 T. From linear polarised chromism measurements, absorption measurements were made with a polariser placed parallel (Fig. 5(b)) and perpendicular (Fig. 5(c)) to the direction of the applied magnetic field of the sample. The absorption intensity in the direction perpendicular to the magnetic field ( $B_{\perp}$ ) was larger than that in the parallel direction ( $B_{\parallel}$ ).  $B_{\perp}$  and  $B_{\parallel}$  correspond to  $Abs_{\parallel}$  and  $Abs_{\perp}$ , respectively, where  $Abs_{\perp}$  and  $Abs_{\parallel}$  represent absorbance perpendicular and parallel to the main chain, respectively. The vibrational direction of incident light corresponds to the direction of the polymer orientation that results in strengthening of the optical absorption intensity in  $Abs_{\parallel}(B_{\perp})$ , which indicates that the transition dipole moment of the conjugated segment is perpendicular to the direction of the applied magnetic field (the main chain is oriented perpendicular to the magnetic field). The dichroic ratio ( $R$ ) and order parameter ( $S$ ) at the maximum absorption wavelength for the synthesised polymers are summarised in Table 1.

Fig. 5.

Table 1.

The  $R$  value of PEDOT-SmA<sub>4T</sub> is estimated to be 2.09 (doping, 0.5 V) and 2.78 (dedoping, -0.8 V), and  $S$  is 0.26 (0.5 V, doping) and 0.37 (-0.8 V, dedoping). The  $R$  and  $S$  values of the electrochemically dedoped species are higher than those of the doped species. Intrusion of dopant into the polymer results in extension of the distance between the main chains, and thus, the orientation becomes somewhat disordered.

The  $R$  and  $S$  values for the polymers are increased with ordering of the electrolyte solution LC phase as a reaction field ( $N < Ch^* < SmA$ ). NLC and Ch\*LC with low order parameters did not provide high orientational molecular ordering for the monomer during polymerisation. The order parameter of the reaction field directly reflects the molecular arrangement of the polymer. The POM images confirm that PEDOT-Ch\*<sub>4T</sub> is more highly oriented than PEDOT-N\*<sub>4T</sub>. In the case of the polymer prepared in Ch\*LC under a magnetic field of 4 T, the fingerprint structure stretched in one-direction along the magnetic field. The oriented direction of the polymer chromophore is in the direction perpendicular to the magnetic field. It should be noted that the polymers thus prepared were very stable at room temperature, with no change in either surface

structure or optical properties after 2 months in the air.

### Reversible polarised optical absorption

Fig. 6 shows the reversible change in the optical absorption spectra with anisotropy at  $\lambda_{\max}$  for the  $\pi$ - $\pi^*$  transition of PEDOT-N<sub>4T</sub> (Fig. 6(a)), PEDOT-Ch\*<sub>4T</sub> (Fig. 6(b)), and PEDOT-SmA<sub>4T</sub> (Fig. 6(c)). This electrochemical redox state-induced change in optical absorption can be reasonably explained as being due to electrochemical doping/dedoping of the main chain, and demonstrates reversible linear polarised electrochromism.

Fig. 6

### Plausible structure

LC can be described as a director field, and the polymer grows along the field to produce macroscopic ordering during polymerisation. The magnetic force orients the director field and polymer growth is oriented according to the director field.

The individual LC molecules in the N, Ch\*, and Sm phases orient along the magnetic field, while the chromophore (main chain) of the polymer orients perpendicular to the direction of the magnetic field. Fig. S15 (Supplementary

Information) shows the molecular arrangement of NLC and Ch\*LC illustrated with directors. The arrangement of the directors of the N phase reflect a schlieren texture under the POM, as shown in Fig. S15(a) (Supplementary Information), and the magnetic orientation aligns the directors, as shown in Fig. S15(b) (Supplementary Information). In the case of Ch\*LC, the vortex (fingerprint) structure under zero magnetic field (Fig. S15(c), Supplementary Information) is transformed to a line texture by the magnetic field, because the helical axis aligns in the direction perpendicular to the direction of the magnetic field, which results in helical half-pitch lines of the polymer arranged along the magnetic field (Fig. S15(d), Supplementary Information). The magnitude of the magnetic field is less than that of the critical magnetic field ( $B_c$ ).<sup>[35]</sup> In this case, PEDOT grows across the direction of the oriented molecules; therefore, the oriented direction of the chromophore (PEDOT main chain) is perpendicular to the direction of the applied magnetic field.

The polymer prepared in SmA shows distinct aligned domains and a fibril structure. Fig. 7(a) shows a plausible internal structure of the SmA phase with a focal conic fan-shaped texture, where thick lines indicate the layer boundaries. The local structure of SmA is shown in Fig. 7(b), which corresponds to the arrangement shown in Fig. 1(c). Here, Fig. 7(c) shows a POM image of the SmA electrolyte containing the monomer.

Electropolymerisation in the SmA matrix yields a polymer with the characteristic focal conic fan-shaped texture, as schematically depicted by Fig. 7(d). The fibrils of PEDOT grow along the layer boundary of the SmA matrix during polymerisation (Fig. 7(e)). This process affords PEDOT with focal conic fan-shaped texture, as shown by the POM image in Fig. 7(f). This structure is in good agreement with the theoretically predicted ellipsoid model of the SmA phase.<sup>[11]</sup> The molecular arrangement of the SmA phase with polygonal texture is illustrated in Fig. S16 (Supplementary Information). Electropolymerisation of *ter*EDOT in the polygonal texture is performed in the LC domain, and results in fibril structures. Polymerisation under a magnetic field creates oriented domains of SmALC (Fig. 8(a)). SEM observation reveals that the PEDOT fibrils grow in the direction perpendicular to the domains (Fig. 8(b)). The fibrils (Fig. 8(c)), can be thought of as molecular cables that make up the main chains of PEDOT (Fig. 8(d,e)).

Lastly, it should be noted that the transcription from the solvent did not occur in the isotropic state of SmA and in acetonitrile solution, which indicates that isotropic solutions are invalid for preparation of the polymer with ordered structure, whereas the LC electrolytes in the LC temperature range play the role of exact molecular templates.

Fig. 7

Fig. 8

## Conclusion

Electropolymerisations under magnetic field in LC were carried out under a magnetic field. The polymers were imprinted with the molecular arrangement of the LCs, and the fibrils of the polymers align perpendicular to the applied magnetic field. The direction of alignment is determined by the macroscopic orientation of the LC electrolyte solution matrix during the polymerisation process. The polymer exhibits a reversible change in polarised optical absorption with electrochemical doping/dedoping. This phenomenon can be referred to as linear polarised electrochromism.

## Chemicals

*ter*EDOT was synthesised by the previously reported method.<sup>[30]</sup> 4-Hydroxy cyanobiphenyl, K<sub>2</sub>CO<sub>3</sub>, and 1-octylbromide were purchased from Tokyo Kasei Japan (TCI). 4-hexyl-4'-cyanobiphenyl was obtained from Merck (USA). Ethanol, acetone, ether (Wako, Japan) were used as received.

## Technique

Magnetic orientation was carried out with a drum type cryogen-free superconducting magnet (Japan Magnet Technology, JMT). Absorption spectra were obtained using a UV-Vis spectrophotometer (Hitachi U-2000). Electrochemical measurements of polymers were conducted using an electrochemical analyser ( $\mu$ Autolab III, Autolab, Netherlands), and optical textures were observed using a high-resolution polarising microscope (Nikon ECLIPS LV 100) with a Nikon LU Plan Fluor and Nikon CFIUW lenses at 500 $\times$  and 1000 $\times$  magnification without oil immersion.

### **Acknowledgments**

The author is grateful to the Engineering Workshop of the University of Tsukuba for glasswork. NMR measurements were carried out by the Chemical Analysis Division of the Research Facility Centre for Science and Technology, University of Tsukuba. The drum type magnet was provided by National Institute for Materials Science (NIMS), Japan. We thank to K. Kawabata (U. Tsukuba) for his kind assistance of illustrations preparation.



## References

- [1] R. A. Potyrailo, H. Ghiradella, A. A. Vertiatchikh, K. Dovidenko, J. Cournoyer, E. Olson, *Nat. Photonics*, 2007, **1**, 123.
- [2] A. Tsuruma, M. Tanaka, S. Yamamoto, N. Fukushima, H. Yabu, M. Shimomura, *Colloids Surf., A*, 2006, **470**, 284.
- [3] (a) H. Goto, *Adv. Func. Mater.*, 2009, **19**, 1335. (b) Jpn Pat., 2008-32415 (Feb 13, 2008).
- [4] I. Mogi, K. Watanabe, M. Motokawa, *Physica B*, 1998, **246–247**, 412.
- [5] T. Kimura, T. Kawai, Y. Sakamoto, *Polymer*, 2000, **41**, 809.
- [6] H. Yonemura, Y. Yamamoto, S. Yamada, Y. Fujiwara, Y. Tanimoto, *Sci. Technol. Adv. Mat.*, 2008, **9**, 024213.
- [7] J. Wang, M. Scampicchio, R. Laocharoensuk, F. Valentini, O. Gonzalez-Garca, J. Burdick, *J. Am. Chem. Soc.*, 2006, **128**, 4562.
- [8] M. S. Cho, Y. Y. Yun, J. D. Nam, Y. Son, Y. Lee, *Synth. Met.*, 2008, **158**, 1043.
- [9] The aromatic rings are aligned parallel to the magnetic field.
- [10] H. Goto, S. Nimori, K. Akagi, *Synth. Met.*, 2005, **155**, 576.

- [11] D. Demus, L. Richter. *Texture of liquid crystals*, Verlag Chemie, Weinheim, New York, 1978.
- [12] I. Dierking, L. L. Kosbar, A. Afzali-Ardakani, A. C. Lowe, G. A. Held, *J. Appl. Phys.*, 1997, **81**, 3007.
- [13] G. A. Held, L. L. Kosbar, I. Dierking, A. C. Lowe, G. Grinstein, V. Lee, R. D. Miller, *Phys. Rev. Lett.*, 1997, **79**, 3443.
- [14] H. Kihara, T. Miura, *Polymer*, 2005, **46**, 10378.
- [15] H. Kihara, T. Miura, R. Kishi, T. Yoshida, M. Shibata, R. Yosomiya, *Liq. Cryst.*, 2003, **30**, 799.
- [16] H. Kihara, T. Miura, R. Kishi, *Macromol. Rapid Commun.*, 2004, **53**, 445.
- [17] K. Araya, A. Mukoh, T. Narahara, H. Shirakawa, *Chem. Lett.*, 1984, 1141.
- [18] K. Araya, A. Mukoh, T. Narahara, H. Shirakawa, *Synth. Met.*, 1986, **14**, 199.
- [19] H. Shirakawa, K. Akagi, S. Katayama, K. Araya, A. Mukoh, T. Narahara, *J. Macromol. Sci. Pure Appl. Chem.*, 1988, **A25**, 643.
- [20] K. Akagi, S. Katayama, H. Shirakawa, K. Araya, A. Mukoh, T. Narahara, *Synth. Met.*, 1987, **17**, 241.
- [21] K. Akagi, H. Shirakawa, K. Araya, A. Mukoh, T. Narahara, *Polym. J.*, 1987, 185.
- [22] K. Akagi, G. Piao, S. Kaneko, K. Sakamaki, H. Shirakawa, M. Kyotani, *Science*,

- 1998, **282**, 1683.
- [23] (a) H. Goto, K. Akagi, Book of Abstracts of the International Conference of Science and Technology of Synthetic Metals; Research Center for Theoretical Physics of Fudan University: Shanghai, China., 2002, 17; (b) H. Goto, K. Akagi, Jpn. Pat. 362979, **2002**; *Chem. Abstr.*, 2003, **139**, 344169.
- [24] L. Huang, Z. Wang, H. Wang, X. Cheng, A. Mitra, Y. Yan, *J. Mater. Chem.*, 2002, **12**, 388.
- [25] D. Kim, J. Choi, K. J.-Y. Kim, Y. K. Han, D. Sohn, *Macromolecules*, 2002, **35**, 5314.
- [26] C. Li, M. Numata, T. Hasegawa, T. Fujisawa, S. Haraguchi, K. Sakurai, S. Shinkai, *Chem. Lett.*, 2005, **34**, 1532.
- [27] F. Hulvat, S. I. Stupp, *Adv. Mat.*, 2004, **16**, 589.
- [28] D. Wasserberg, S. C. J. Meskers, R. A. J. Janssen, E. Mena-Osteritz, P. Bäuerle, *J. Am. Chem. Soc.*, 2006, **128**, 17007.
- [29] G. A. Sotzing, J. R. Reynolds, P. J. Steel, *Adv. Mater.*, 1997, **9**, 795.
- [30] H. Goto, *J. Mater. Chem.*, 2009, **19**, 4914.
- [31] H. Goto, *Phys. Rev. Lett.*, 2007, **98**, 253901.
- [32] (a) H. Yoneyama, R. Ohta, H. Goto, *Macromolecules*, 2007, **40**, 5279; (b) G.

Solladie', G. Zimmermann, *Angew. Chem. Int. Ed. Engl.*, 1984, **23**, 348.

[33] N. P. M. Huck, W. F. Jaeger, B. Lange, B. L. Fringe, *Science*, 1996, **273**, 1686.

[34] I. Dierking, *Textures of Liquid Crystals*, Wiley-VCH, Weinheim, Germany 2003.

[35] The helical structure of cholesteric liquid crystals unwinds at magnetic fields

higher than  $B_c$ .

## Figure captions

**Table 1.** Dichroic ratio and order parameter of polymers prepared by electropolymerisation under 4 T.

**Fig. 1.** Molecular arrangement of (a) nematic (N), (b) cholesteric (Ch\*) phase, and (c) smectic A (SmA) phases. (d) Sandwich cell electropolymerisation method. (e) Detachment of the cell after polymerisation.

**Fig. 2.** POM images of electrochemically prepared PEDOT in LC under magnetic field with insertion of gypsum first-order red plate (LC free samples). (a) PEDOT prepared in NLC electrolyte under zero magnetic field (PEDOT-N<sub>0T</sub>). (b) PEDOT prepared by electropolymerisation in NLC electrolyte under 4 T (PEDOT-N<sub>4T</sub>). (c) PEDOT prepared by electropolymerisation in Ch\*LC electrolyte under 4 T (PEDOT-N<sub>4T</sub>).

**Fig. 3.** (a,b) POM images of PEDOT (LC free sample) prepared in SmA under zero magnetic field. (b) Insertion of gypsum first-order red plate. (c,d) SEM image of the

polymer. (a,c) Polygonal texture at different locations in the sample. (b,d) Focal conic fan-shaped texture at different locations in the sample. (e) SEM image of the polymer taken from a direction oriented  $35^\circ$  from the surface.

**Fig. 4.** Surface images of electrochemically prepared PEDOT in SmA with insertion of gypsum first-order red plate under 4 T (LC free sample) (PEDOT-SmA<sub>4T</sub>). (a) POM image. (b,c) SEM image.

**Fig. 5.** Spectro-electrochemical analysis of PEDOT prepared in SmA (PEDOT-SmA<sub>4T</sub>). (a) Optical absorption during the oxidation (doping) process without polariser. Inset shows optical absorption up to long wavelength. (b) Optical absorption during the oxidation (doping) process with the polariser set perpendicular to the direction of the oriented chromophore ( $Abs_{\perp}$ ,  $B_{\parallel}$ ). (c) Optical absorption during the oxidation (doping) process with the polariser set parallel to the direction of the oriented chromophore ( $Abs_{\parallel}$ ,  $B_{\perp}$ ).

**Fig. 6.** Reversible change in optical absorption for applied voltage between  $-0.8$  and  $0.5$  V. Polymer prepared (a) in NLC under 4 T (PEDOT-N<sub>4T</sub>), (b) in Ch\*LC under 4 T

(PEDOT-Ch\*<sub>4T</sub>), and (c) in SmALC under 4 T (PEDOT-SmA<sub>4T</sub>). Red lines: optical absorbance of the direction parallel to the orientation direction of the polymers (perpendicular to the magnetic field). Blue lines: optical absorbance of the direction perpendicular to the orientation direction of the polymers (parallel to the magnetic field).

**Fig. 7.** Molecular aggregation structure for SmA and PEDOT prepared in SmALC electrolyte solution. (a) Internal structure of focal conic fan-shaped texture. (b) Local molecular arrangement of SmA layer structure. (c) POM image of SmA electrolyte solution containing monomer. (d) Fibril structure of PEDOT prepared in SmA. (e) Local structure of PEDOT prepared in SmA. (f) POM image of PEDOT with focal conic fan-shaped texture prepared in SmA.

**Fig. 8.** Plausible structure of PEDOT prepared in SmALC electrolyte solution under magnetic field. (a) POM image of PEDOT prepared in SmALC under 4 T (PEDOT-SmA<sub>4T</sub>). (b) Magnified SEM image of PEDOT-SmA<sub>4T</sub>. (c) Schematic illustration of the oriented fibril structure. (d) Microfibrils consist of individual PEDOT chains. (e) Chemical structure of PEDOT in the fibrils.



For TOC

The electrochemical preparation of (PEDOT) from *ter*EDOT is conducted in liquid crystalline electrolyte solution under a magnetic field to afford polymer films with linear polarised electrochromism.



**Table 1.** Table 1. Dichroic ratio and order parameter of polymers

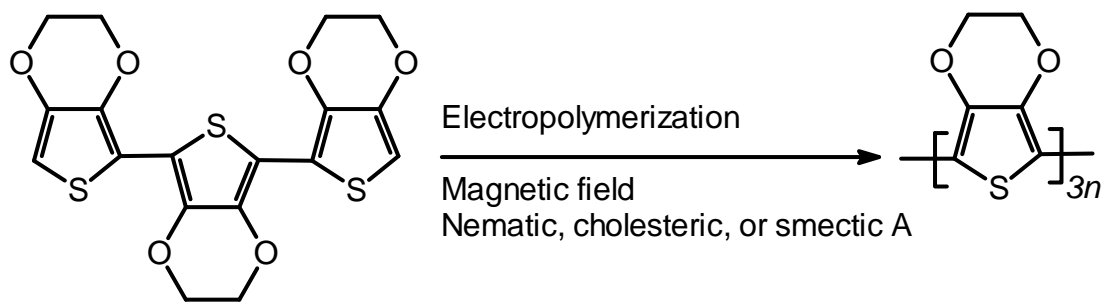
prepared by electropolymerisation under 4 T.

Polymer	Elyte <sup>1</sup>	$R^2$		$S^3$	
		Dope	Dedope	Dope	Dedope
PEDOT-N <sub>4T</sub>	Nematic	1.12	1.17	0.038	0.053
PEDOT-Ch* <sub>4T</sub>	Cholesteric	1.45	1.58	0.13	0.16
PEDOT-SmA <sub>4T</sub>	Smectic A	2.09	2.78	0.26	0.37

<sup>1</sup>Electrolyte solution.

<sup>2</sup>Dichroic ratio ( $R = A_{\parallel} / A_{\perp}$ ).

<sup>3</sup>Order parameter ( $S = (R - 1) / (R + 2)$ )



Polymer <sup>1</sup>	Elyte <sup>2</sup>	$B$ (T) <sup>3</sup>	Matrix LC	Monomer <sup>5</sup>
PEDOT-N <sub>0T</sub>		0		
PEDOT-N <sub>4T</sub>	Nematic <sup>1</sup>	4	(6CB)	
PEDOT-Ch* <sub>0T</sub>		0		
PEDOT-Ch* <sub>2T</sub>		2	(6CB)	
PEDOT-Ch* <sub>4T</sub>	Cholesteric <sup>1</sup>	4		
PEDOT-Ch* <sub>9T</sub>		9	Cholesteryl pelargonate <sup>4</sup>	
PEDOT-SmA <sub>0T</sub>		0		
PEDOT-SmA <sub>4T</sub>	Smectic A <sup>1</sup>	4	(6CB)	
PEDOT-SmA <sub>0T</sub> iso	Smectic A (isotropic, 80 °C) <sup>6</sup>	0		
			(8OCB)	
PEDOT-ACN <sup>6</sup>	Acetonitrile <sup>7</sup>	0	–	

<sup>1</sup>Applied voltage: 4 V, 30 min, supporting salt = tetrabutylammonium perchlorate (TBAP) at room temperature (LC state).

<sup>2</sup>Electrolyte solution

<sup>3</sup>Magnetic field in the course of polymerisation.

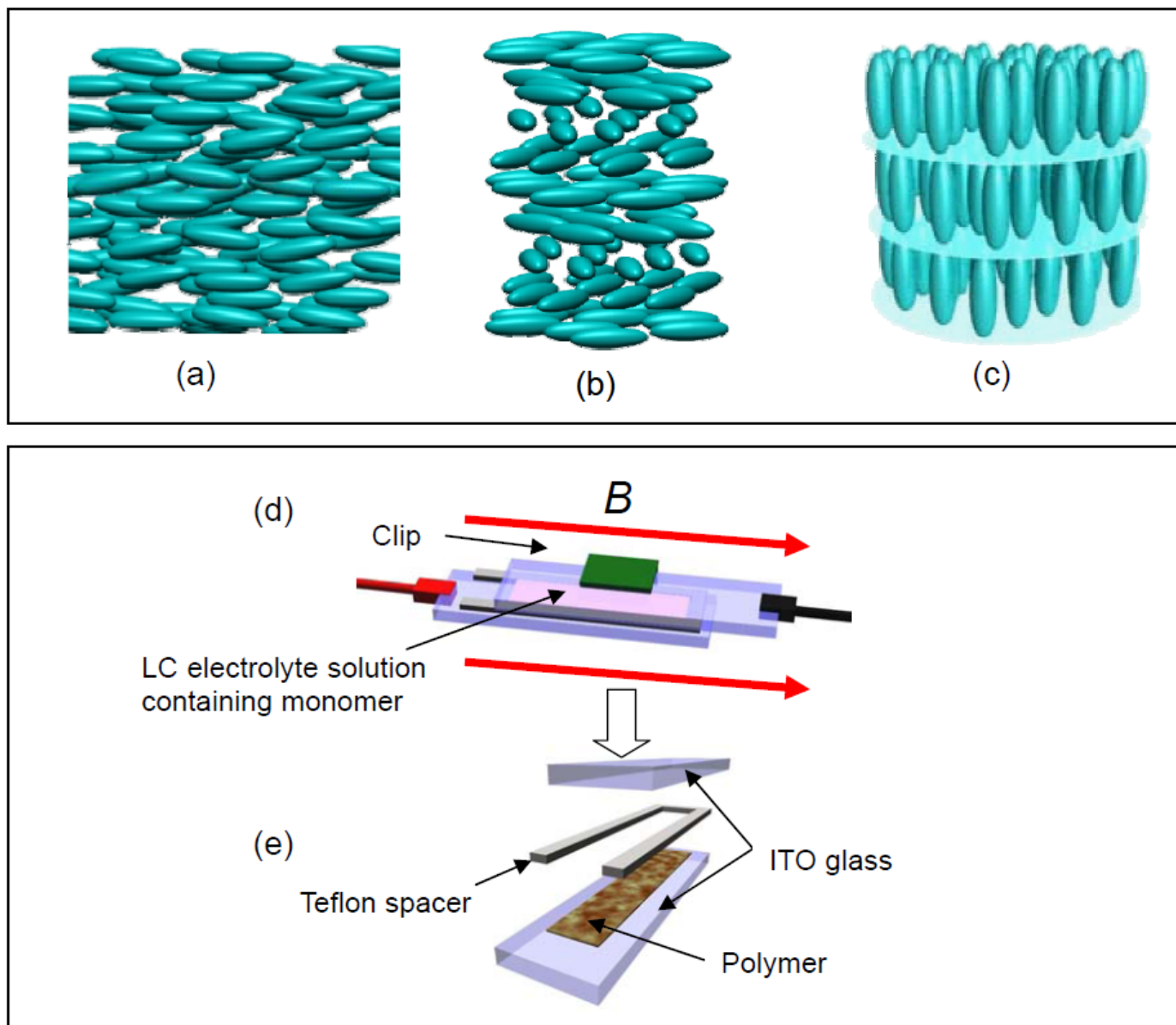
<sup>4</sup>Chiral inducer

<sup>5</sup>terEDOT

<sup>6</sup>Applied voltage: 4 V, 30 min, supporting salt = TBAP at 80 °C

<sup>7</sup>ACN = acetonitrile, CV electrochemical polymerisation in 0.1 M TBAP, scan rate = 50 mV/s, monomer = 0.01 M.

**Scheme 1.**



**Scheme 1.**

**Fig. 1.** Molecular arrangement of (a) N, (b) Ch\*, and (c) SmA LC phases. (d) Sandwich cell electropolymerisation method. (e) Detachment of the cell after polymerisation.

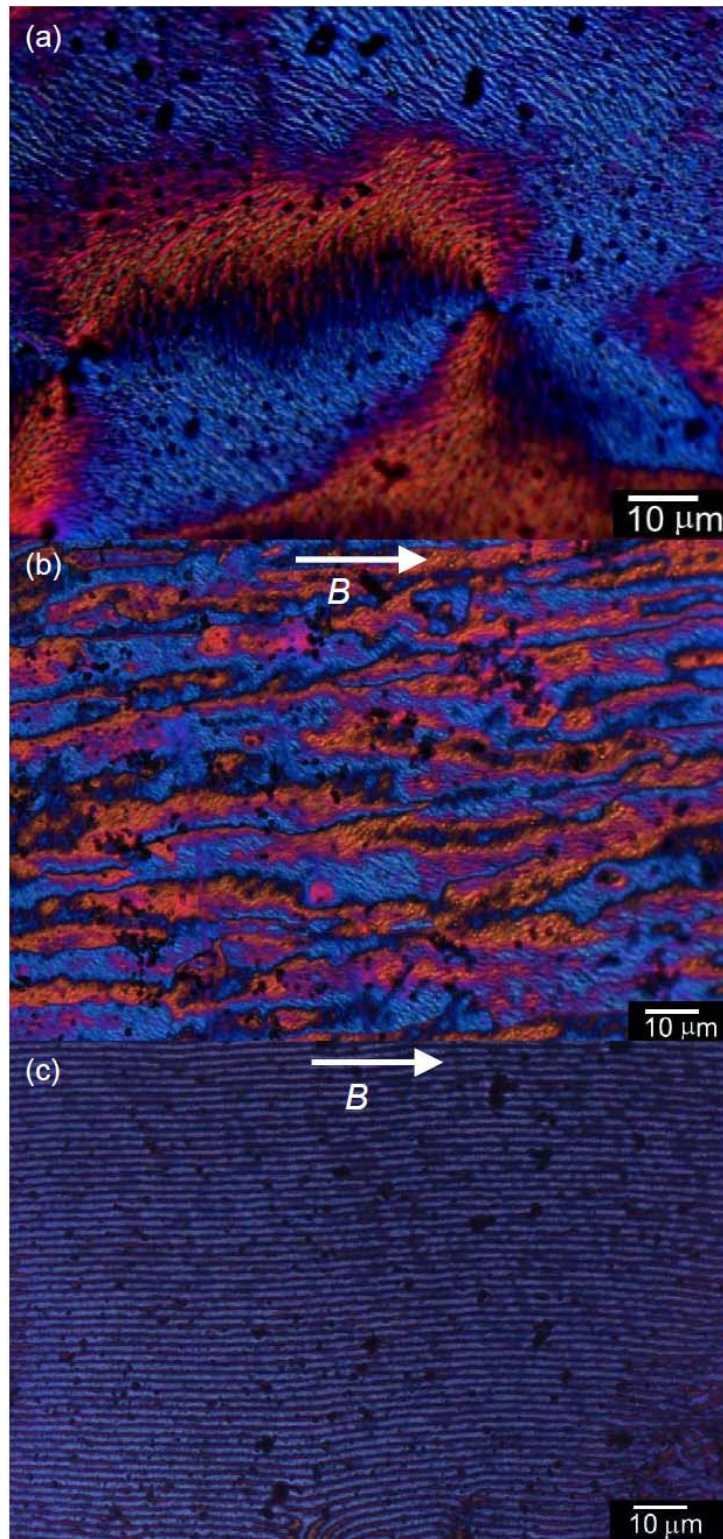


**Fig. 2.** POM images of electrochemically prepared PEDOT in LC under magnetic field with insertion of gypsum first-order red plate (LC free samples). (a) PEDOT prepared in NLC electrolyte under zero magnetic field (PEDOT- $N_{0T}$ ). (b) PEDOT prepared by electropolymerisation in NLC electrolyte under 4 T (PEDOT- $N_{4T}$ ). (c) PEDOT prepared by electropolymerisation in Ch\*LC electrolyte under 4 T (PEDOT- $N_{4T}$ ).

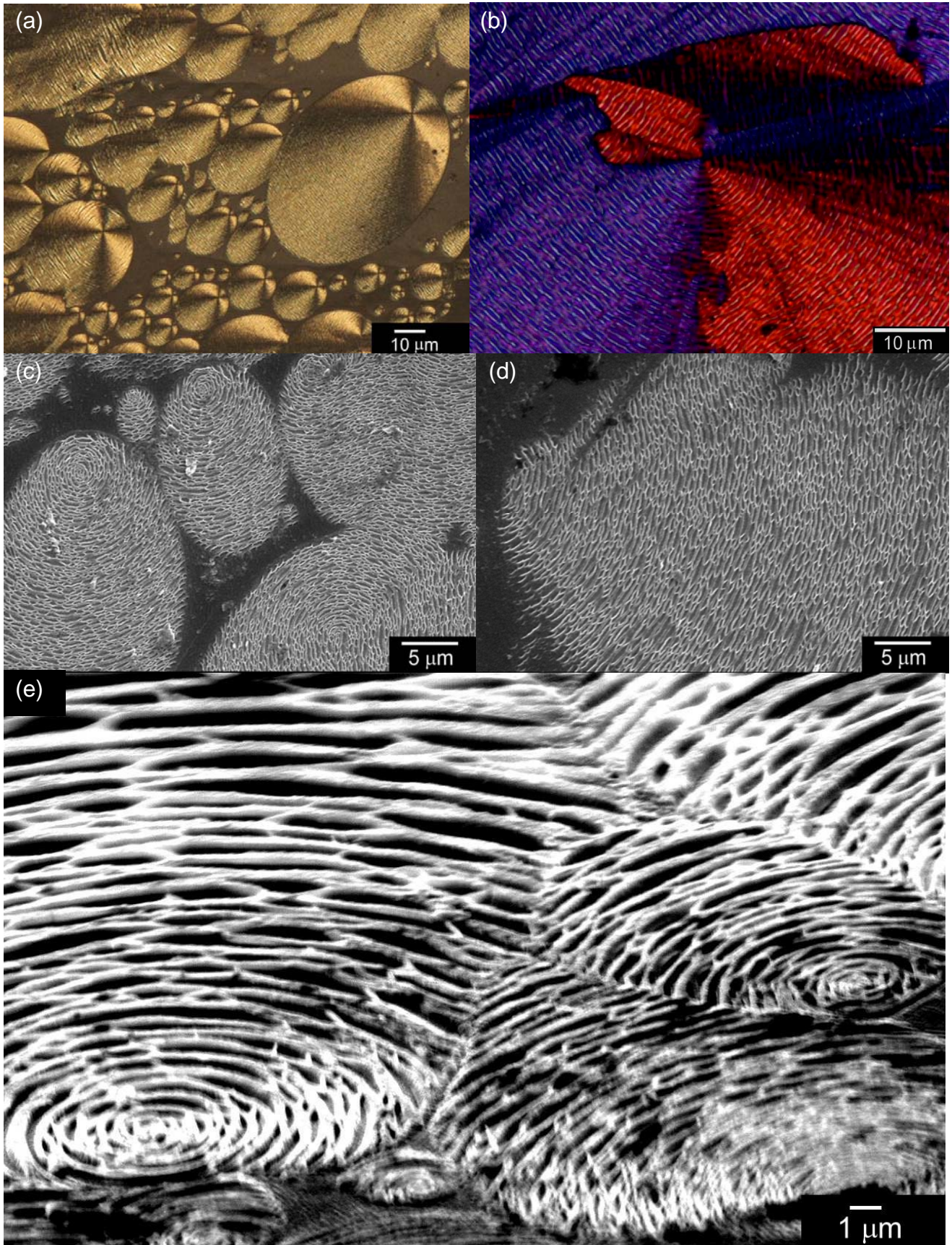


**Fig. 3.** (a,b) POM images of PEDOT (LC free sample) prepared in SmA under zero magnetic field. (b) Insertion of gypsum first-order red plate. (c,d) SEM images of the polymer. (a,c) Polygonal texture at different locations in the sample. (b,d) Focal conic fan-shaped texture at different locations in the sample. (e) SEM image of the polymer taken from a direction oriented  $35^\circ$  from the surface.

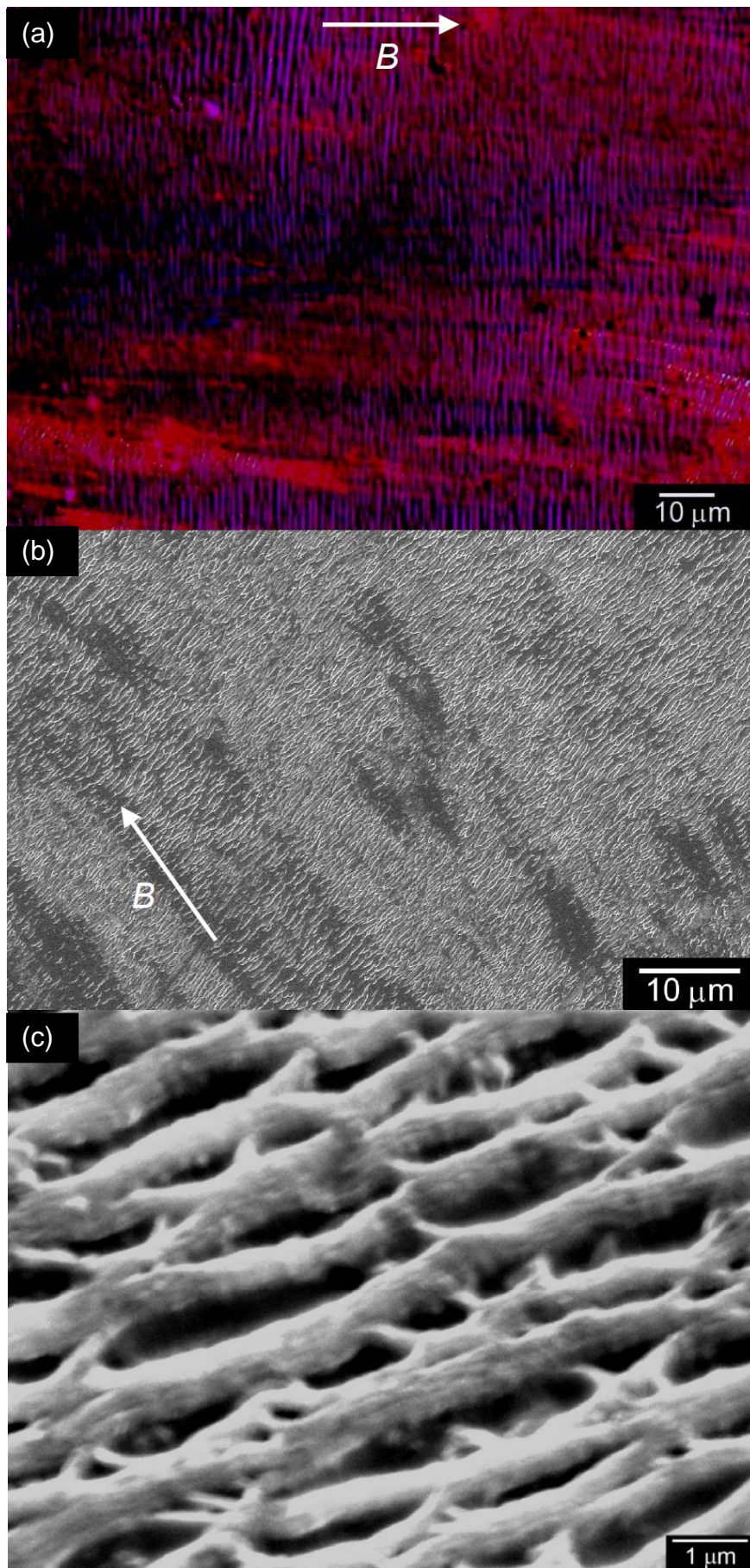


**Fig. 4.** Surface images of electrochemically prepared PEDOT in SmA with insertion of gypsum first-order red plate under 4 T (LC free sample) (PEDOT-SmA<sub>4T</sub>). (a) POM image. (b,c) SEM image.

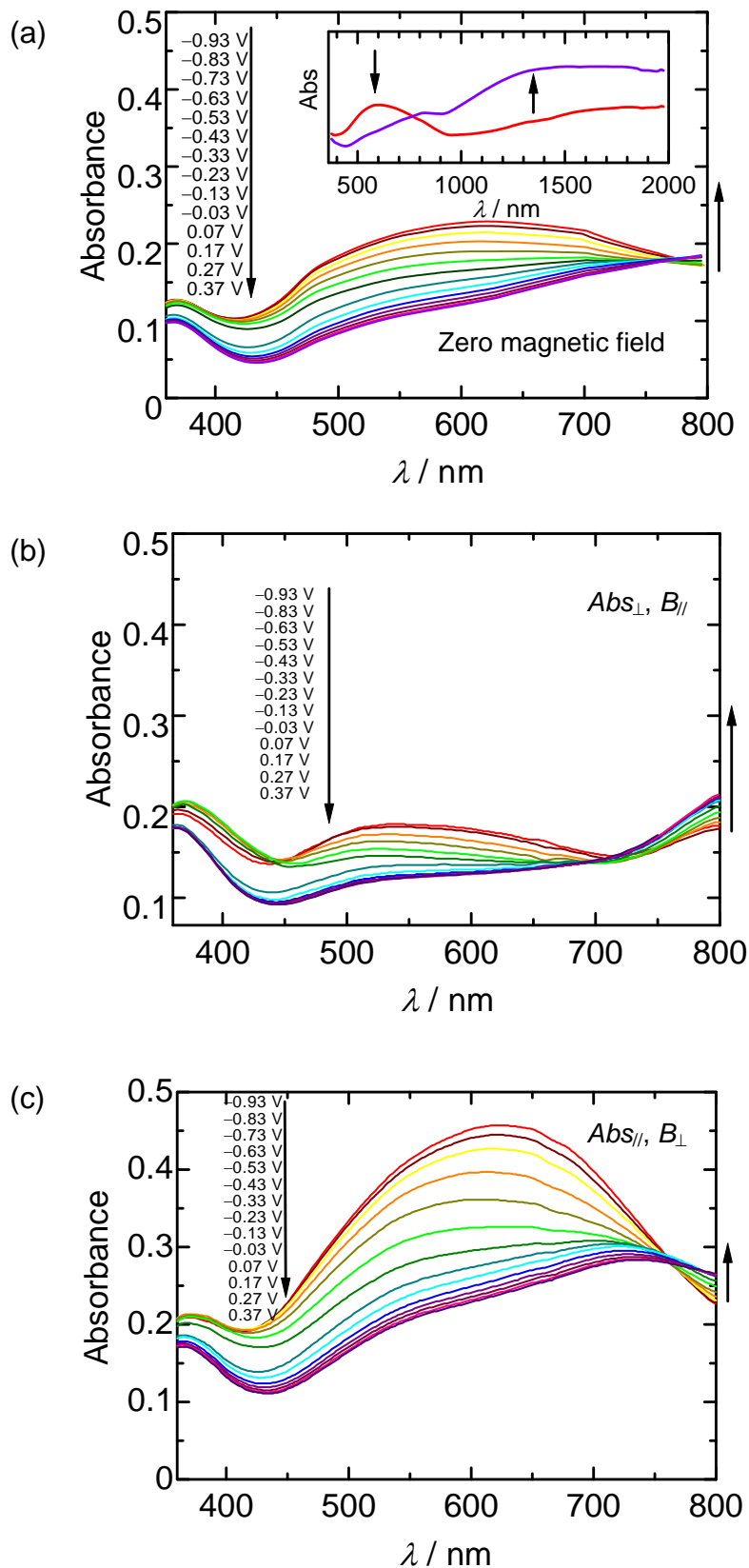


**Fig. 5.** Spectro-electrochemical analysis of PEDOT prepared in SmA (PEDOT-SmA<sub>4T</sub>). (a) Optical absorption during the oxidation (doping) process without polariser. Inset shows optical absorption up to long wavelength. (b) Optical absorption during the oxidation (doping) process with the polariser set perpendicular to the direction of the oriented chromophore ( $Abs_{\perp}, B_{\parallel}$ ). (c) Optical absorption during the oxidation (doping) process with the polariser set parallel to the direction of the oriented chromophore ( $Abs_{\parallel}, B_{\perp}$ ).

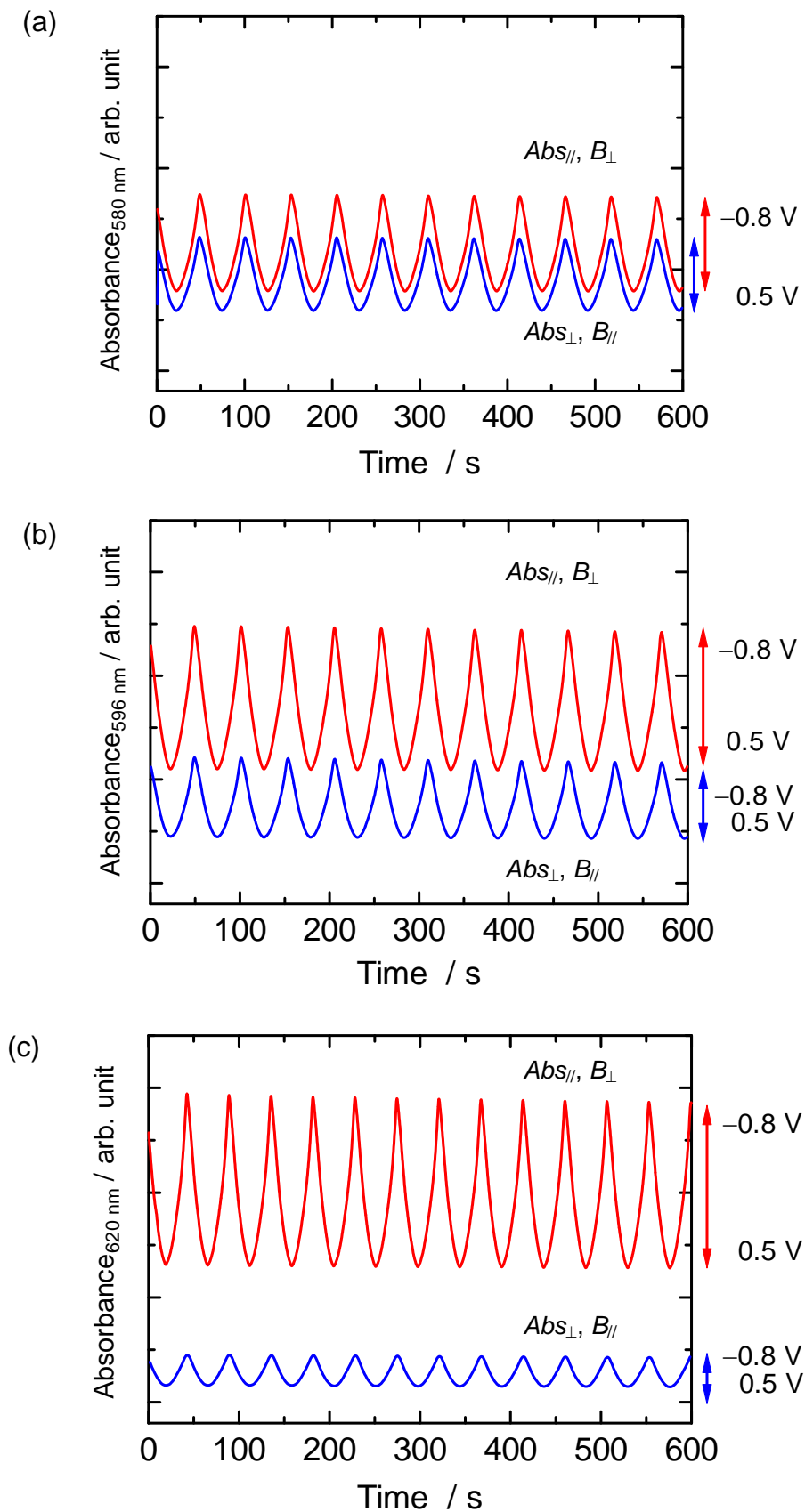


**Fig. 6.** Reversible change in optical absorption for applied voltage between  $-0.8$  and  $0.5$  V. Polymer prepared (a) in NLC under 4 T (PEDOT- $N_{4T}$ ), (b) in  $Ch^*LC$  under 4 T (PEDOT- $Ch^*_{4T}$ ), and (c) in  $SmALC$  under 4 T (PEDOT- $SmA_{4T}$ ). Red lines: optical absorbance of the direction parallel to the orientation direction of the polymers (perpendicular to the magnetic field). Blue lines: optical absorbance of the direction perpendicular to the orientation direction of the polymers (parallel to the magnetic field).



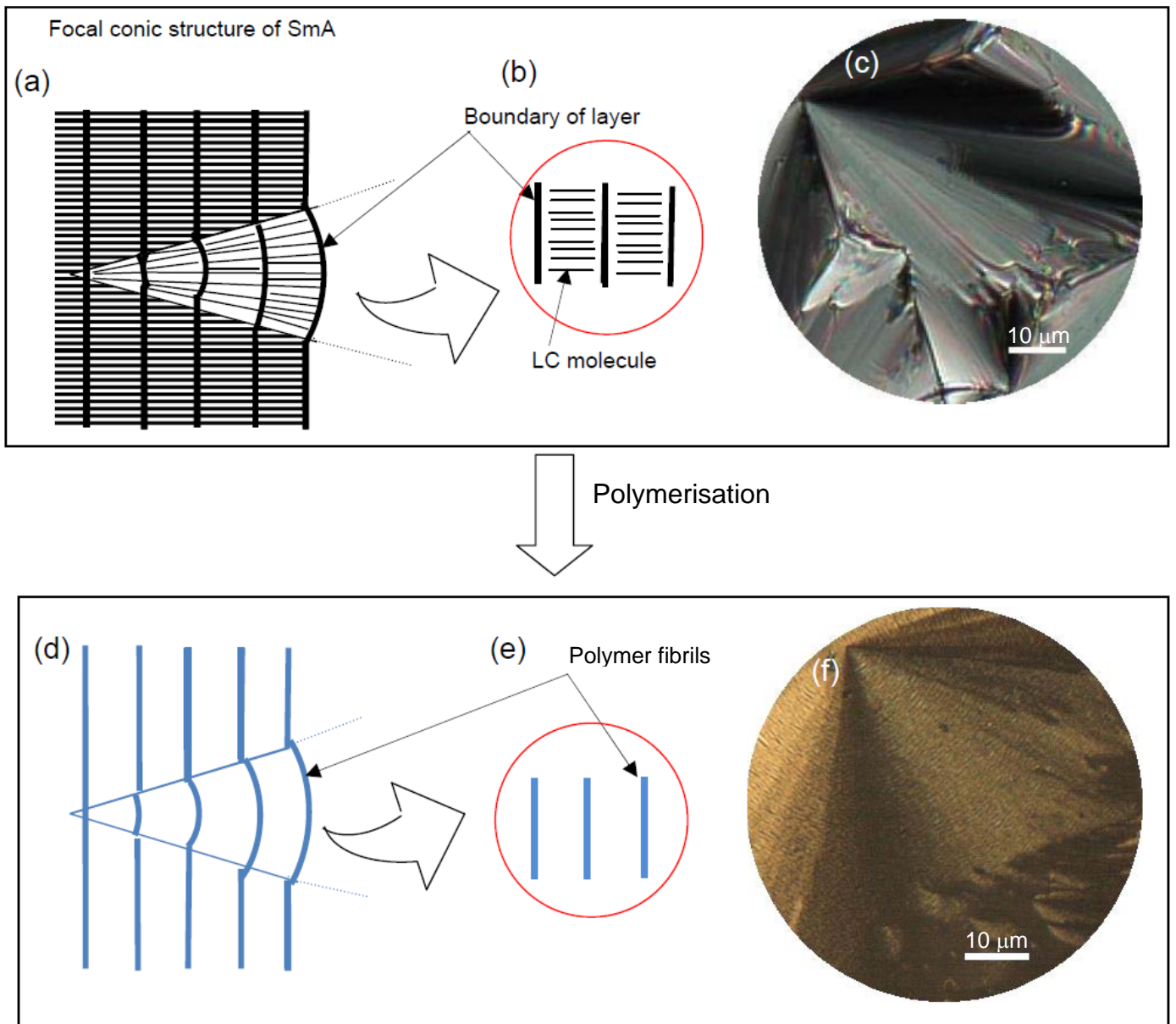


**Fig. 7.** Molecular aggregation structure for SmA and PEDOT prepared in SmALC electrolyte solution. (a) Internal structure of focal conic fan-shaped texture. (b) Local molecular arrangement of SmA layer structure. (c) POM image of SmA electrolyte solution containing monomer. (d) Fibril structure of PEDOT prepared in SmA. (e) Local structure of PEDOT prepared in SmA. (f) POM image of PEDOT with focal conic fan-shaped texture prepared in SmA.

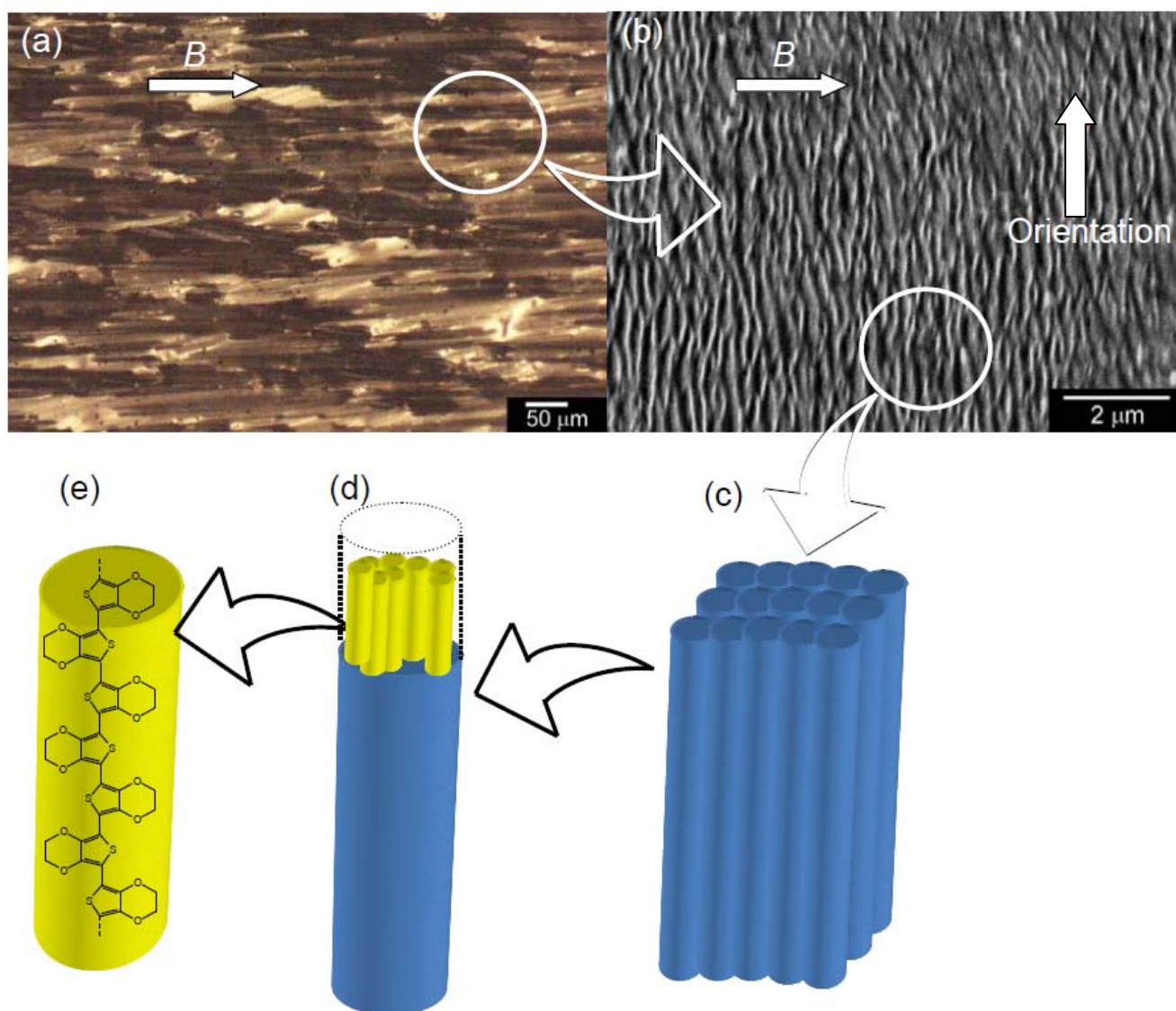


**Fig. 8.** Plausible structure for PEDOT prepared in SmALC electrolyte solution under magnetic field. (a) POM image of PEDOT prepared in SmALC under 4 T (PEDOT-SmA<sub>4T</sub>). (b) Magnified SEM image of PEDOT-SmA<sub>4T</sub>. (c) Schematic illustration of the oriented fibril structure. (d) Microfibrils consist of individual PEDOT chains. (e) Chemical structure of PEDOT in the fibrils.

*Supplementary information for*

Liquid Crystal Electropolymerisation Under Magnetic Field and Resultant Linear  
Polarised Electrochromism

Hiromasa Goto,<sup>1,\*</sup> Shigeki Nimori<sup>2</sup>

<sup>1</sup>Graduate School of Pure and Applied Sciences, Institute of Materials Science, University of Tsukuba, Tsukuba, Ibaraki 305-8573, Japan

<sup>2</sup>National Institute for Materials Science (NIMS), Tsukuba Magnet Laboratory, Sakura, Tsukuba 3-13, Japan

\*Correspondence to H. Goto  
Tel: +81-298-53-5128, fax: +81-298-53-4490  
Email: gotoh@ims.tsukuba.ac.jp

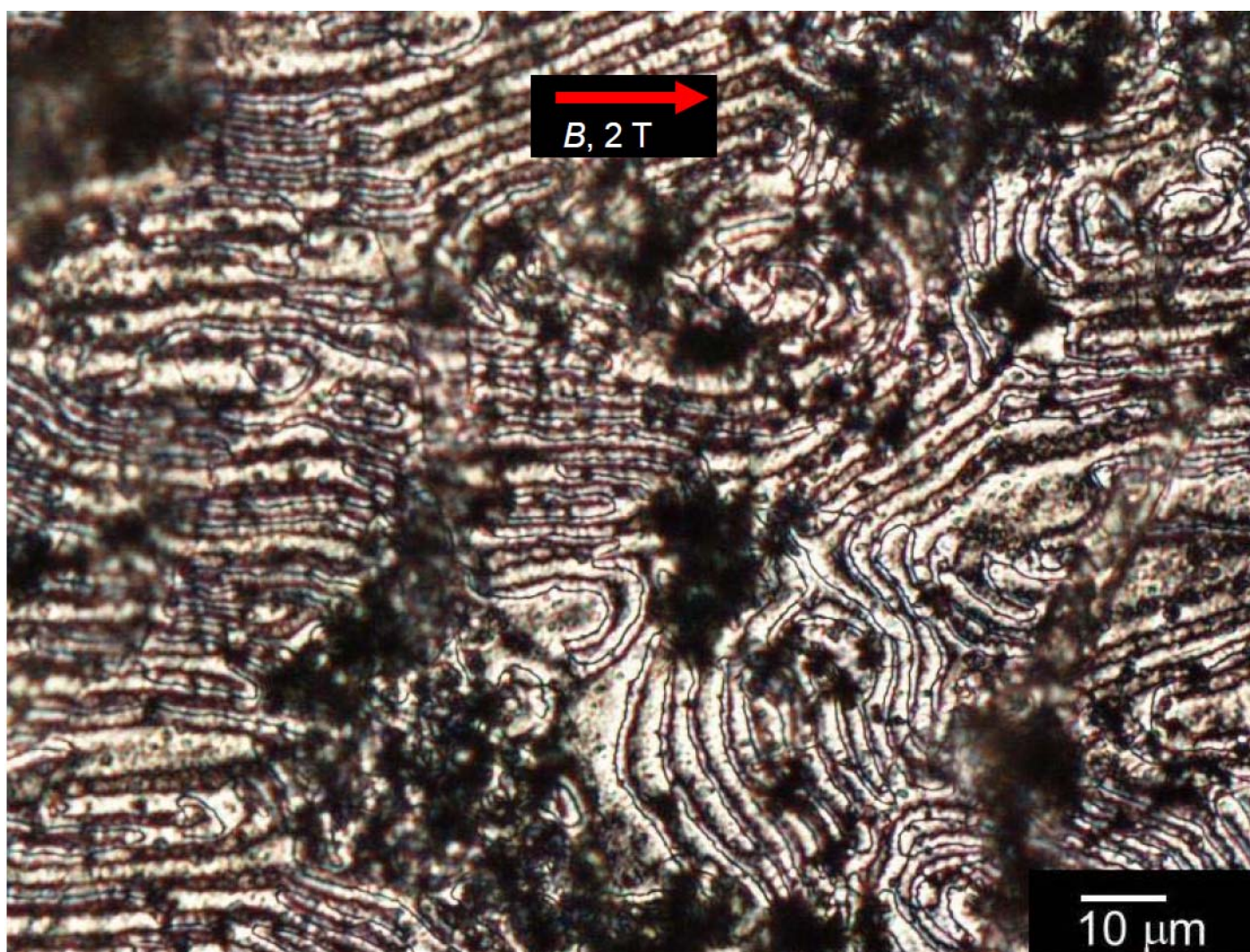


**Fig. S1.** Polarising optical microscopic image of PEDOT prepared in Ch\*LC electrolyte under magnetic field of 2 T (PEDOT-Ch\*<sub>2T</sub>).

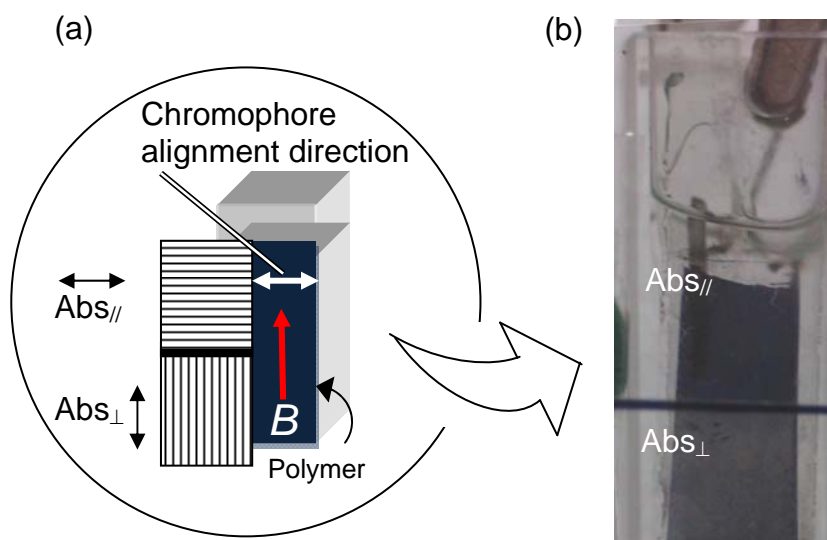


**Fig. S2.** Schematic illustration of PEDOT prepared in SmALC electrolyte under 4 T (PEDOT-SmA<sub>4T</sub>). (a) Direction of the polariser setting for visual observation of the oriented sample. (b) Visual inspection through two polarisers (PEDOT-SmA<sub>4T</sub>) in a quartz cuvette. Abs = absorption.

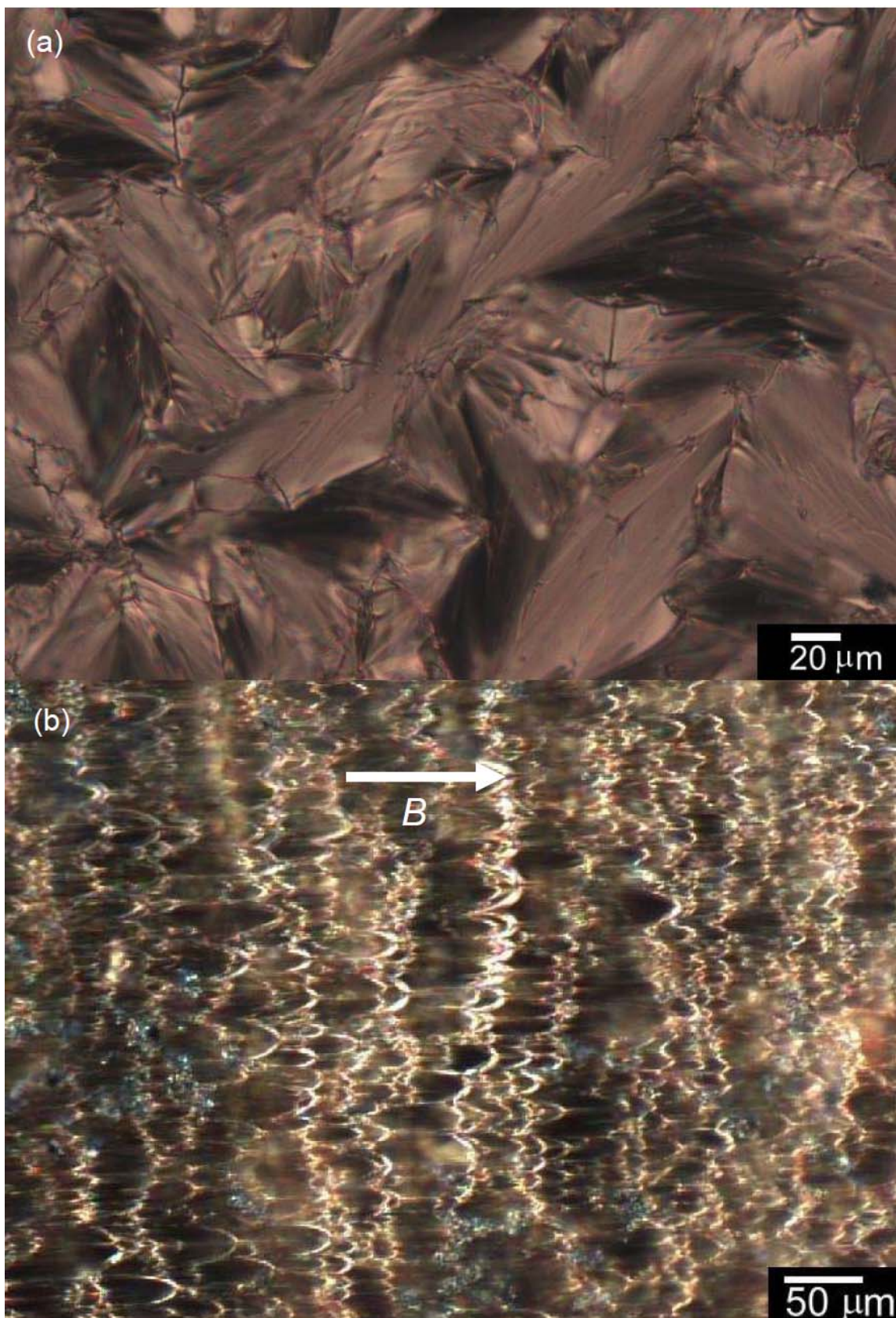


**Fig. S3.** POM images of SmALC electrolyte solution containing the monomer (2,3,2',3',2'',3'-hexahydro-[5,5':7',5'']*ter*[thieno[3,4-b]-[1,4]dioxine]; *ter*EDOT) and supporting salt (tetrabutylammonium perchlorate; TBAP) (a) showing random fan-shaped texture at 25 °C, and (b) under 4 T at 25 °C.

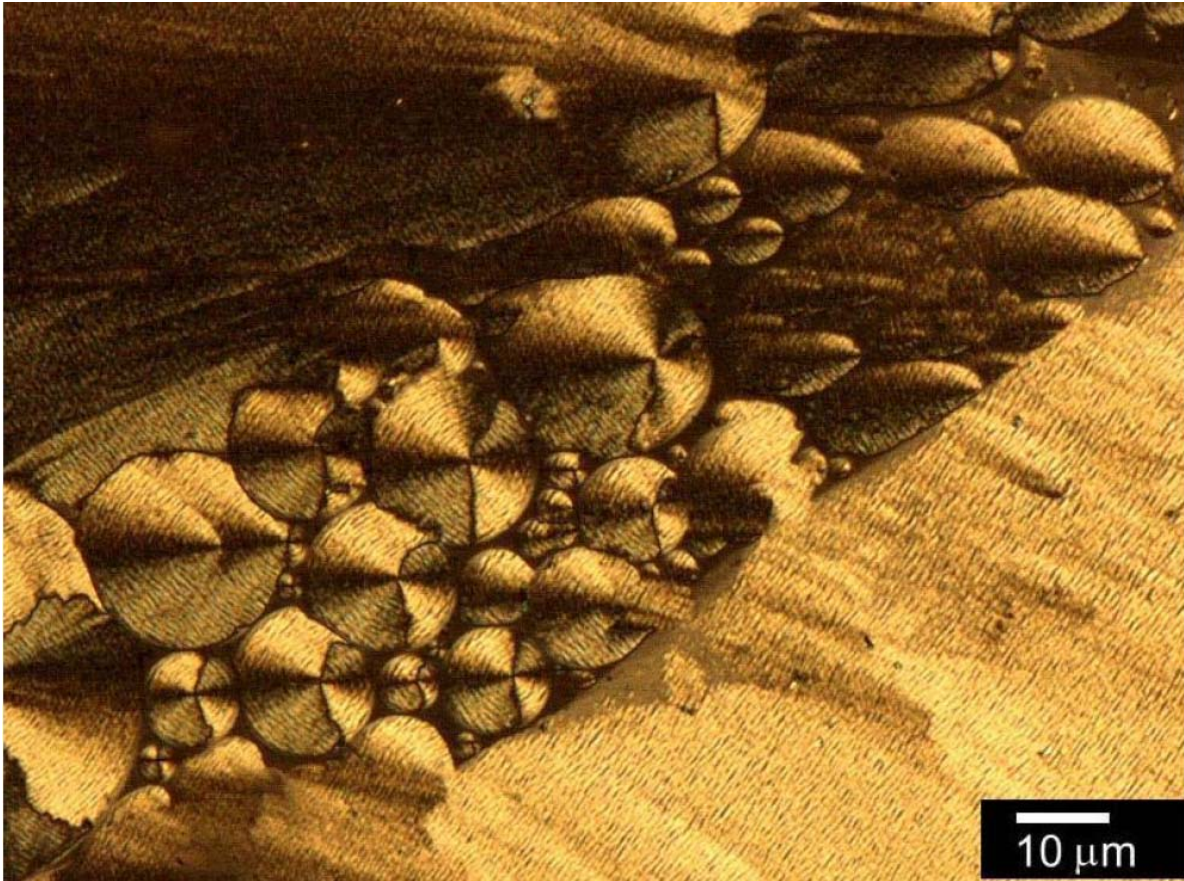


**Fig. S4.** POM image of PEDOT prepared in SmALC electrolyte solution under zero magnetic field, showing multi-domain structure without insertion of gypsum first-order red plate.

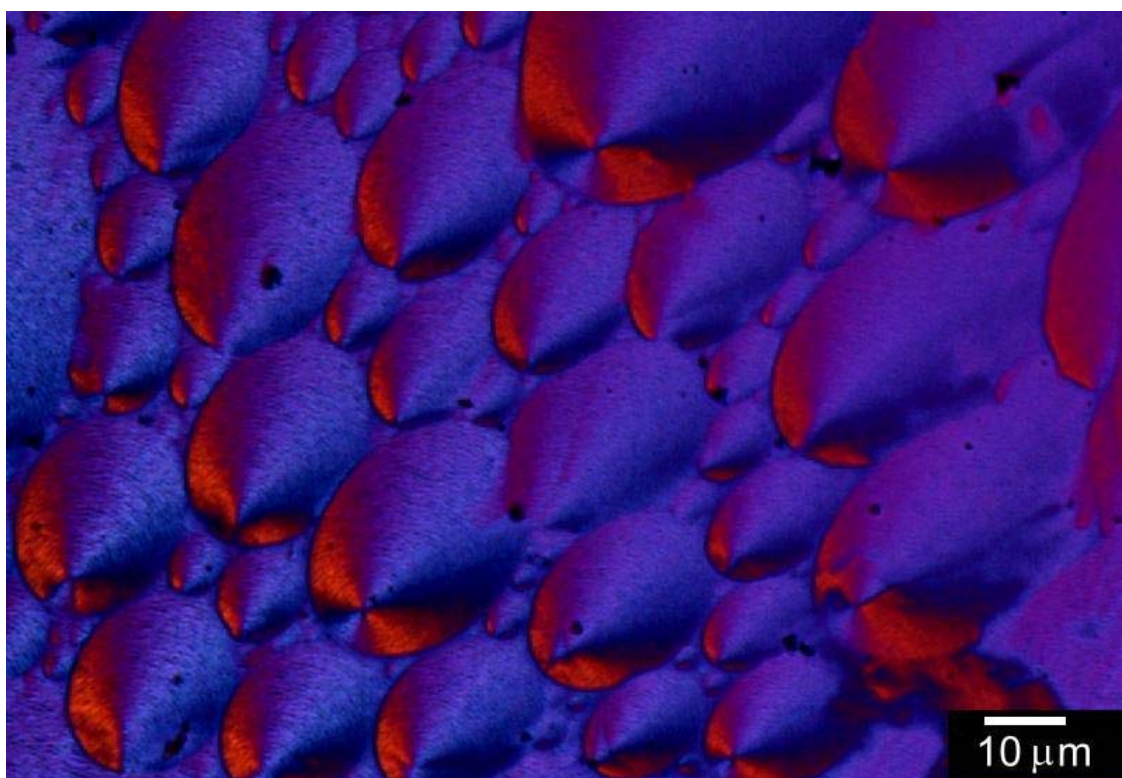


**Fig. S5.** POM images of PEDOT (LC free sample) prepared in SmA with insertion of gypsum first-order red plate under zero magnetic field.



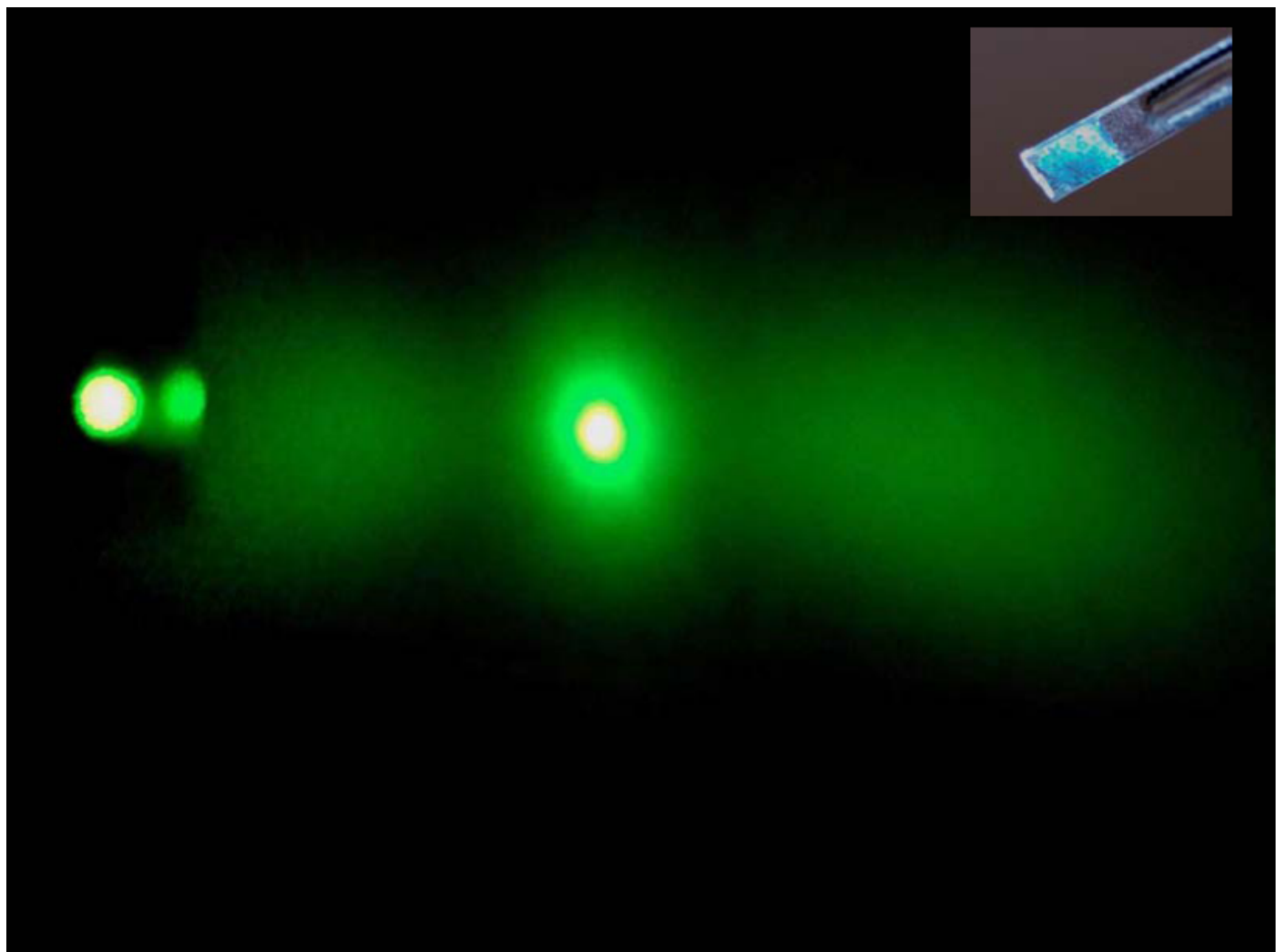


**Fig. S6.** Laser diffraction image of PEDOT prepared in SmALC electrolyte under zero magnetic field (PEDOT-SmA<sub>0T</sub>). Inset shows the reflection colour of PEDOT with an oblique angle of incidence from a white light emitting diode beam.

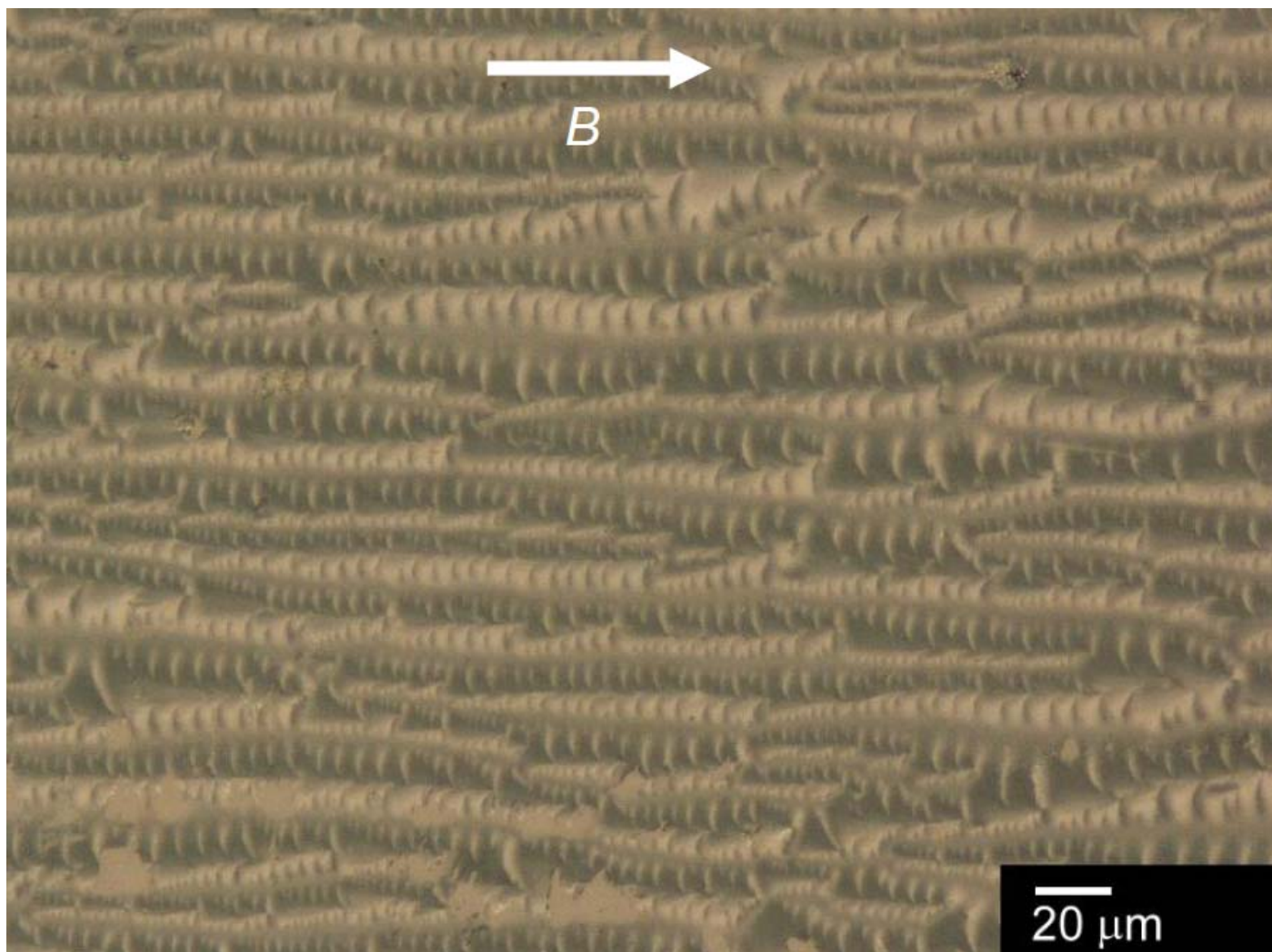


**Fig. S7.** POM image of PEDOT prepared in SmALC electrolyte solution under a magnetic field of 4 T, showing an aloe leaf-like structure.

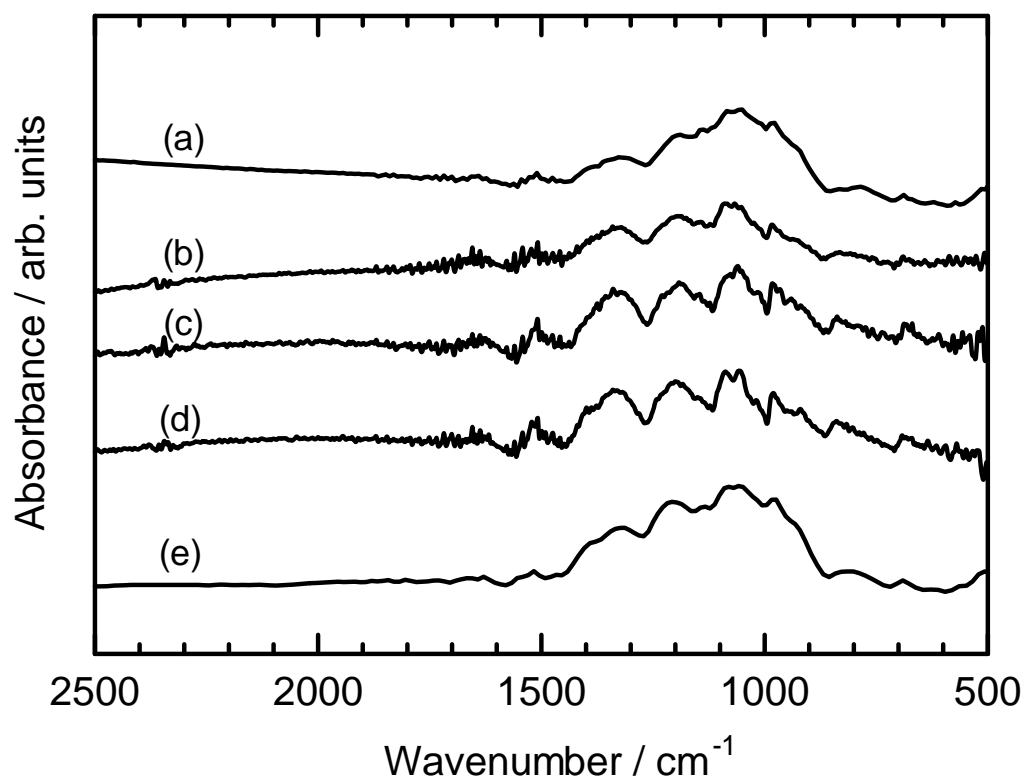


**Fig. S8.** Infrared (IR) spectra of PEDOT prepared in acetonitrile solution (PEDOT-ACN) (a), nematic liquid crystal (LC) (LC free sample) (PEDOT-N<sub>4T</sub>) (b), cholesteric LC (LC free sample) (PEDOT-Ch\*<sub>4T</sub>) (c), smectic A LC (LC free sample) (PEDOT-SmA<sub>4T</sub>) (d), isotropic state of smectic A LC at 80 °C (LC free sample) (PEDOT-SmA<sub>0T</sub>iso) (e).

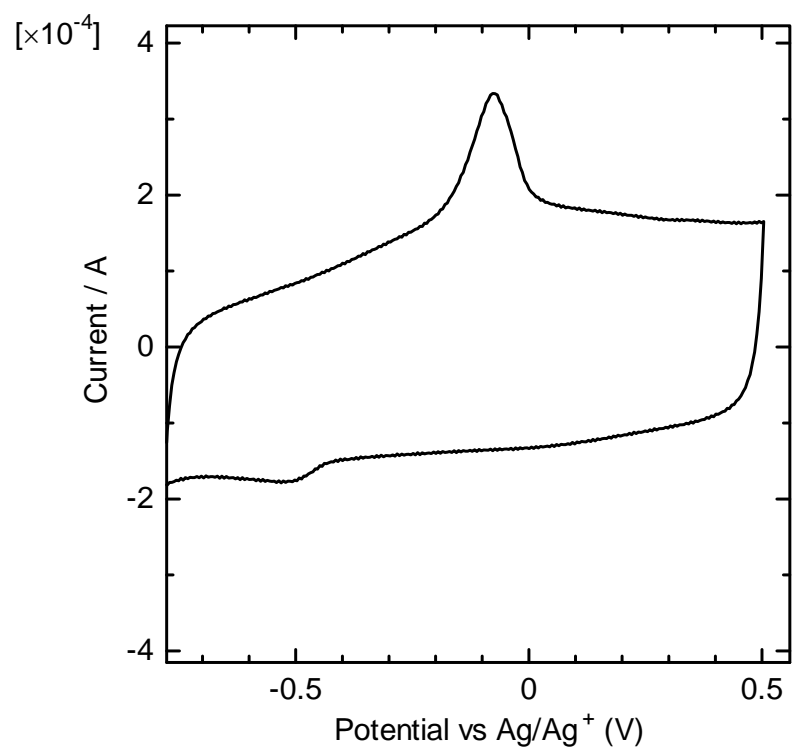


**Fig. S9.** Cyclic voltammogram of PEDOT prepared with SmALC(PEDOT-SmA<sub>4T</sub>) at a scan rate of 100 mV/s in 0.1 M TBAP/acetonitrile solution.

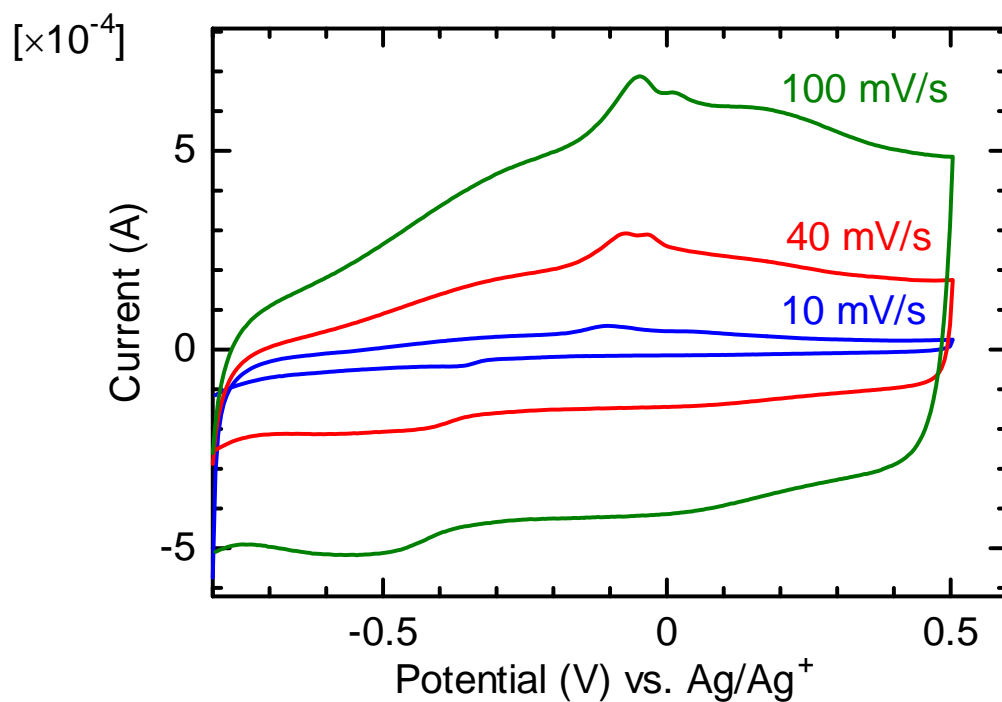
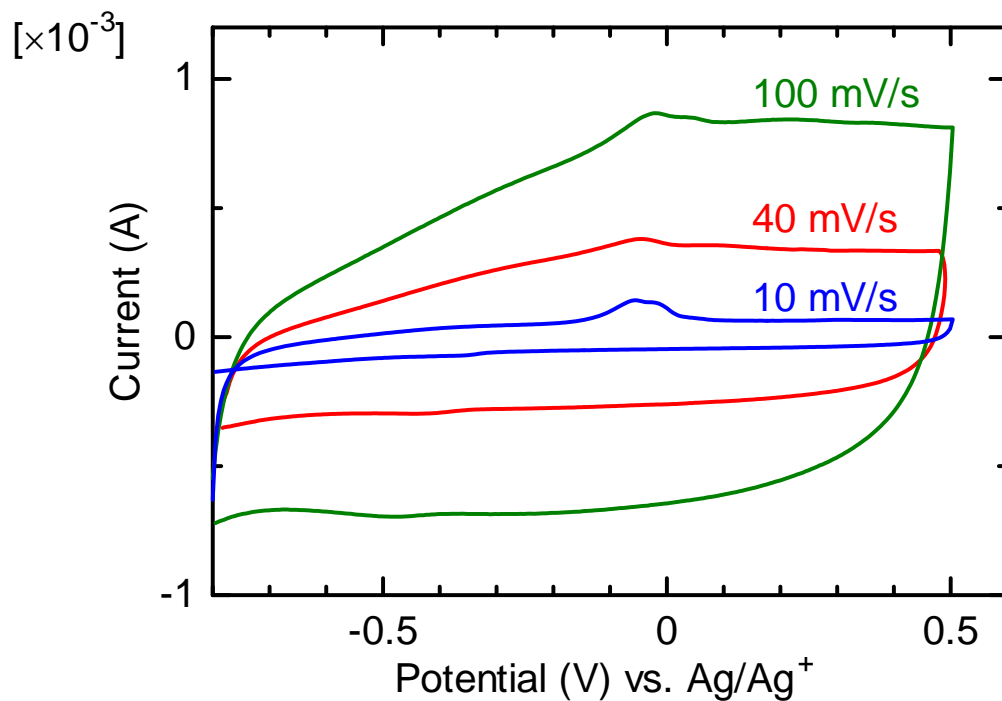


**Fig. S10.** Cyclic voltammogram of PEDOT in monomer free 0.1 M TBAP/acetonitrile solution. (a) PEDOT prepared in acetonitrile solution at room temperature (PEDOT-ACN). (b) PEDOT prepared in isotropic state (80 °C) of SmALC (PEDOT-SmA<sub>0Tiso</sub>).

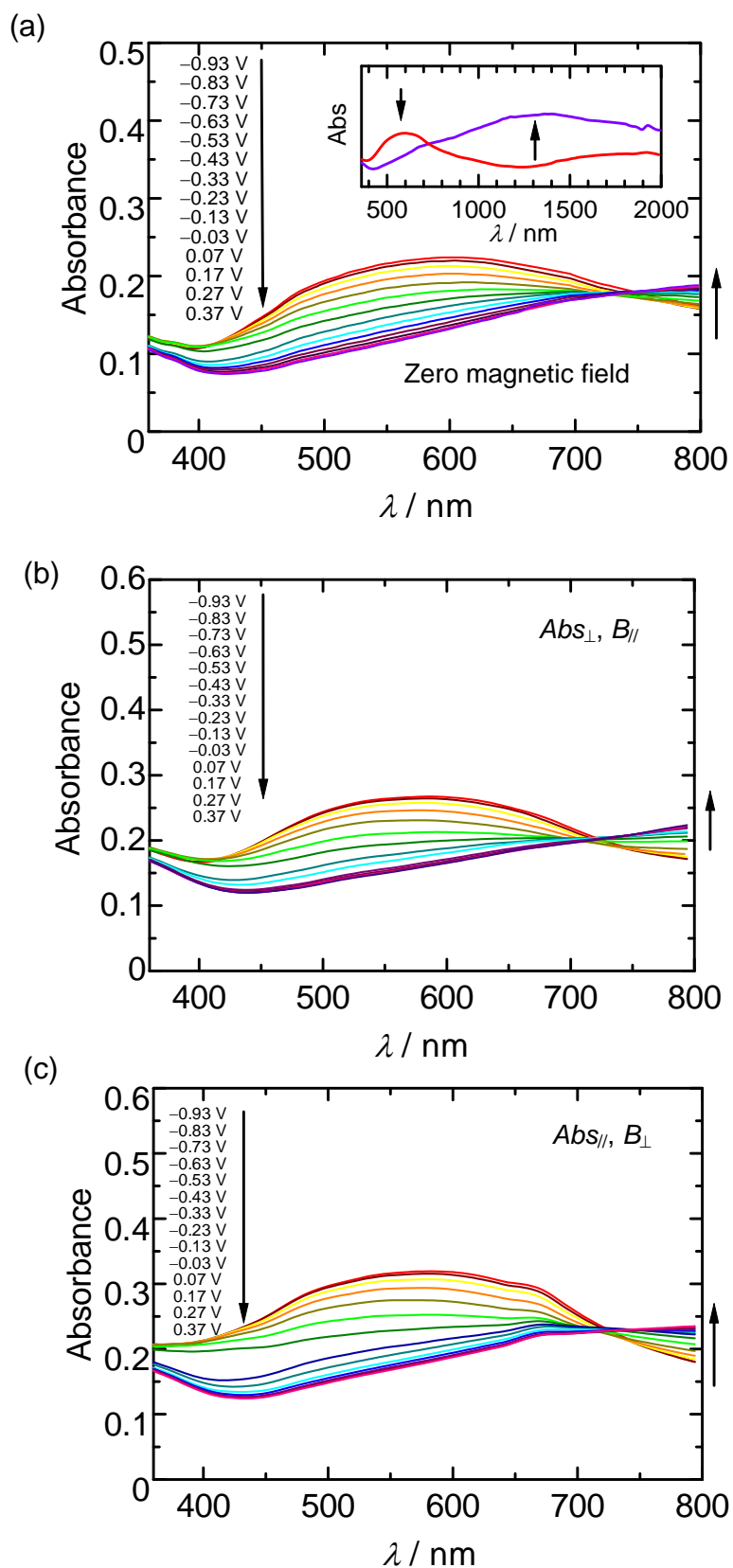


**Fig. S11.** Spectro-electrochemical analysis of PEDOT prepared in NLC electrolyte solution (a) under zero magnetic field and (b,c) under 4 T (PEDOT- $N_{4T}$ ). (a) Change in optical absorption during the doping (oxidation) process without the polariser. The inset shows the optical absorption at long wavelength. (b) Optical absorption during the doping (oxidation) process with the polariser set perpendicular to the direction of the oriented chromophore ( $Abs_{\perp}, B_{\parallel}$ ). (c) Optical absorption during the doping (oxidation) process with the polariser set parallel to the direction of the oriented chromophore ( $Abs_{\parallel}, B_{\perp}$ )

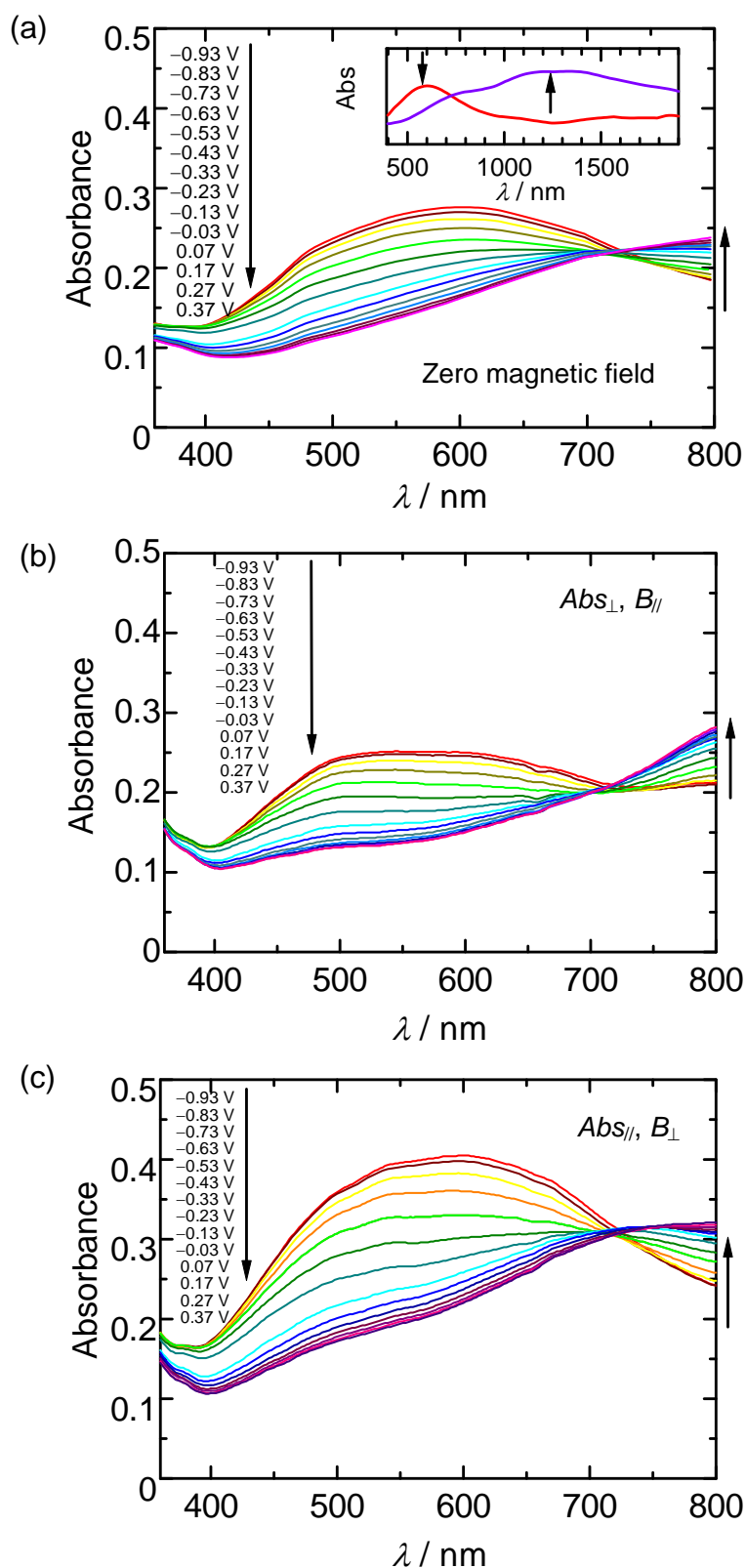


**Fig. S12.** Spectro-electrochemical analysis of PEDOT prepared in Ch\*LC electrolyte solution (a) under zero magnetic field and (b,c) under 4 T (PEDOT-Ch\*<sub>4T</sub>). (a) Optical absorption spectrum during the oxidation (doping) process without the polariser. The inset shows the optical absorption spectrum at long wavelength. (b) Optical absorption spectrum during the oxidation (doping) process with the polariser set perpendicular to the direction of the oriented chromophore ( $Abs_{\perp}, B_{\parallel}$ ). (c) Optical absorption spectrum during the oxidation (doping) process with the polariser set parallel to the direction of the oriented chromophore ( $Abs_{\parallel}, B_{\perp}$ ).

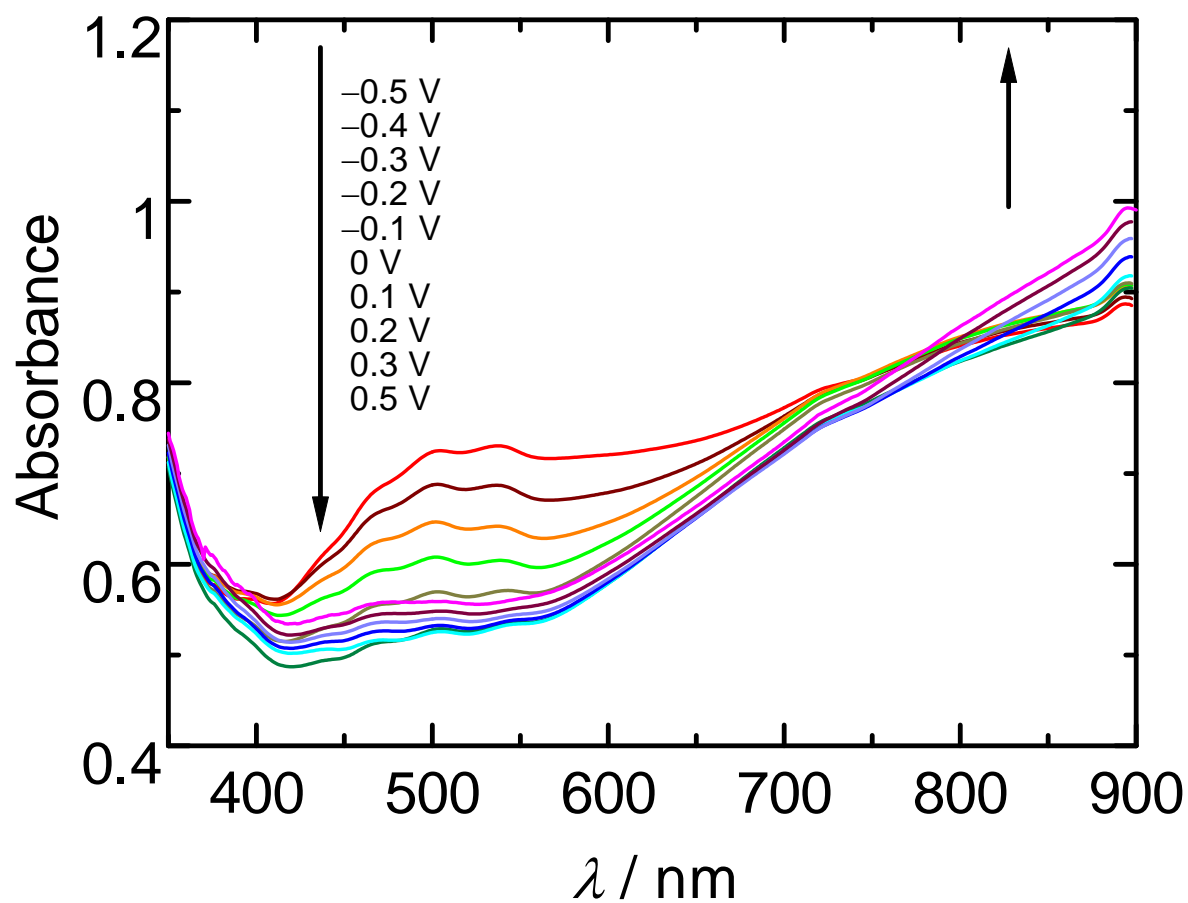


**Figure S13.** Spectro-electrochemical analysis of PEDOT prepared from *ter*EDOT (PEDOT-ACN) in monomer-free 0.1 M acetonitrile solution under zero magnetic field. Optical absorption spectra during the oxidation (doping) process without the polariser.



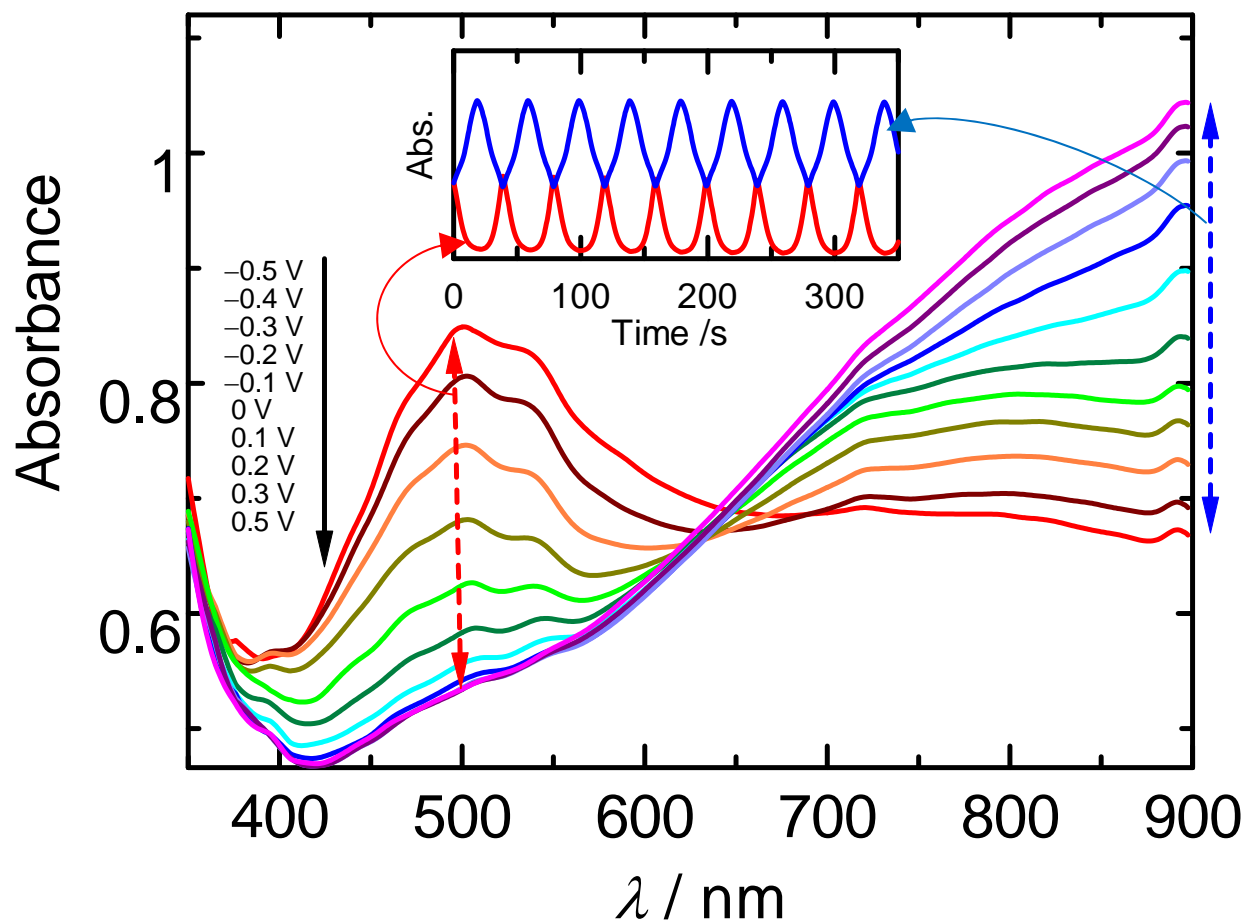


**Figure S14.** Spectro-electrochemical analysis of PEDOT prepared from *ter*EDOT in an isotropic state SmA electrolyte solution under zero magnetic field (PEDOT-SmA<sub>0T</sub>iso) in monomer-free 0.1 M acetonitrile solution (6CB: 0.165 g, 8OCB: 0.33 g, TBAP: 0.25 mg, *ter*EDOT: 2.5 mg). Optical absorption spectra during the oxidation (doping) process without the polariser. The inset shows the reversible change in intensity during the oxidation/reduction (doping/dedoping) process (CV scan, 50 mV/s) at 500 nm (red line) and 900 nm (blue line).

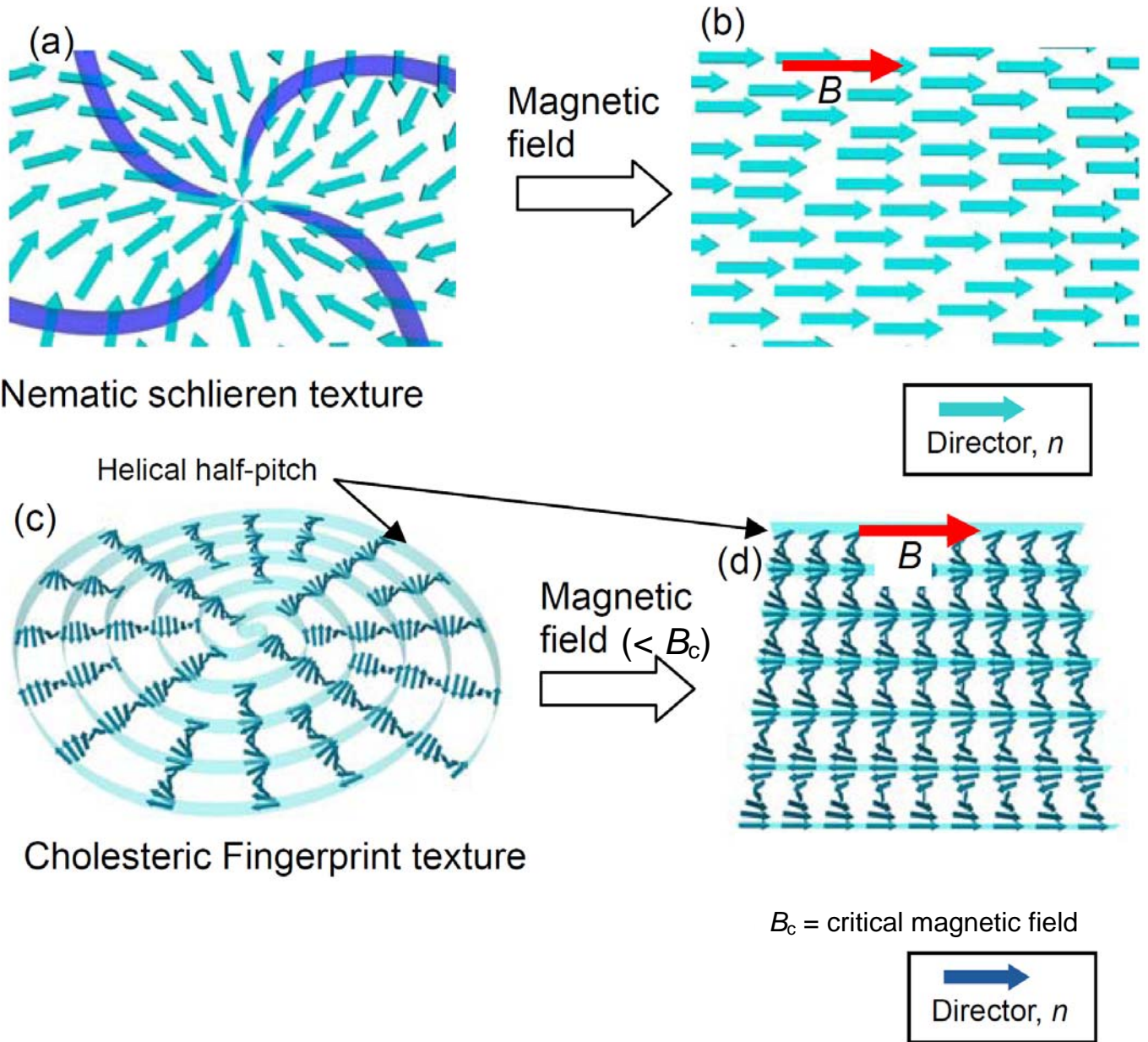


**Fig. S15.** (a) Molecular arrangement of the nematic schlieren texture. (b) Magnetic orientation of NLC. (c) Cholesteric fingerprint texture under zero magnetic field. (d) Magnetic orientation of Ch\*LC ( $< B_c$ ). Magnetic fields higher than  $B_c$  result in unwinding of the helical arrangement of Ch\*LC. Arrows indicate the directors ( $n$ ) of individual molecules in the LC state.

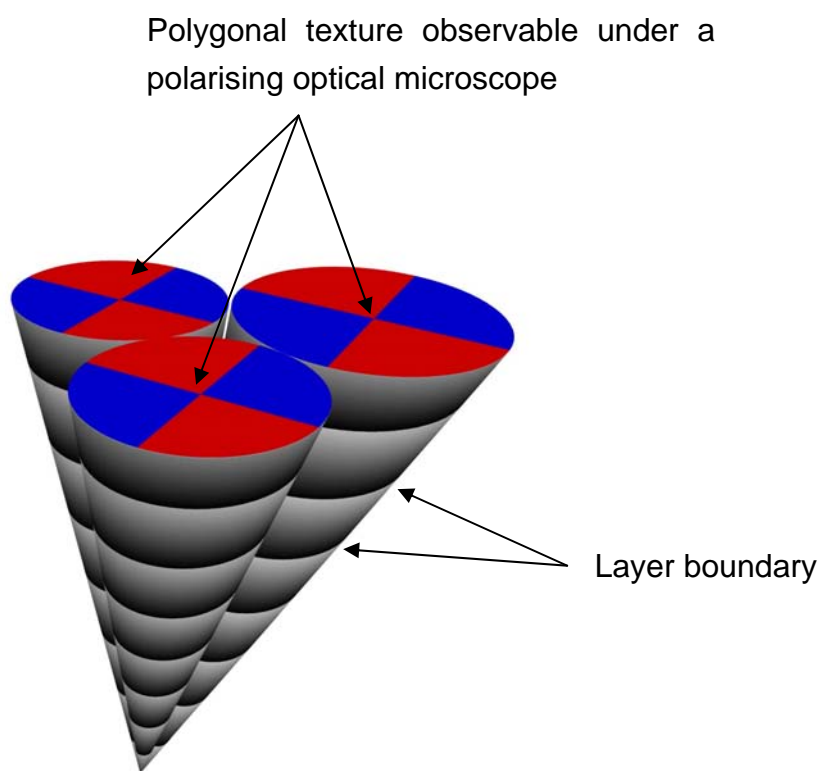


**Fig. S16.** Molecular arrangement of the polygonal texture of the SmA phase.

## Experimental

### 4-Octyloxy-4'-cyanobiphenyl (8OCB):

4-Hydroxy cyanobiphenyl (5 g, 25.6 mmol) and  $K_2CO_3$  (3.5 g, 25.6 mmol) were added to 1-octylbromide (4.95 g, 25.6 mmol) in 30 mL of ethanol. A catalytic amount of dibenzo-crown-6 (1 mg) was added to the solution and the reaction mixture was then stirred and refluxed for 24 h. The reaction mixture was evaporated to remove the solvents, and washed several times with water. The organic layer was extracted with ether. The ether was evaporated and the crude product was recrystallised from acetone to yield 5.2 g of white powder. Yield = 66%.  $^1H$  NMR (500 MHz,  $\delta$  from TMS,  $CDCl_3$ ): 0.89 (3H,  $CH_3$ , t,  $J = 6.0$  Hz), 1.29-1.50 (10H,  $CH_2$ , m), 1.8 (2H,  $OCH_2CH_2$ , quint,  $J = 4.3$  Hz), 4.00 (2H,  $OCH_2$ , t,  $J = 6.4$  Hz), 6.99 (2H, d, ph,  $J = 8.0$  Hz), 7.52 (2H, d, ph,  $J = 7.9$  Hz), 7.64 (2H, d, ph,  $J = 7.9$  Hz), and 7.68 (2H, d, ph,  $J = 7.6$  Hz) ppm.  $^{13}C$  NMR (125 MHz,  $\delta$  from TMS,  $CDCl_3$ ): 14.11, 22.67, 26.05, 29.23, 29.25, 29.36, 31.82, 68.20, 110.03, 115.10, 119.13, 127.08, 128.32, 131.25, 132.57, 145.31, and 159.83 ppm. The NMR spectra are shown in Figure S16 ( $^1H$  NMR) and Figure S17 ( $^{13}C$  NMR) (Supporting Information).

### Preparation of NLC electrolyte solution

NLC electrolyte solution was prepared by dissolving TBAP (0.1 mg) as a supporting salt and *ter*EDOT (monomer, 5 mg) in 6CB (matrix LC, 0.5 g) under argon flow. At room temperature, the NLC electrolyte solution exhibits a schlieren texture, as observed under the POM. The NLC electrolyte solution was heated once in a vial to 40 °C under an argon atmosphere, in order to completely dissolve the supporting salt and monomer in the 6CB LC solvent.

### **Preparation of Ch\*LC electrolyte solution**

Ch\*LC electrolyte solution was prepared with the addition of a small amount of cholesteric pelargonate (an optically active material) as a Ch\*LC inducer to 6CB as an NLC to induce the formation of Ch\*LC with a mesoscopic helical structure.

The Ch\*LC electrolyte solution was prepared as a reaction solvent by the addition of cholesteryl pelargonate (10 mg) to 6CB (0.5 g). TBAP (0.1 mg) was then added as a supporting salt. Liquid crystallinity was confirmed to be maintained after the addition of the monomer (*ter*EDOT, 5 mg). At room temperature, the Ch\* electrolyte solution exhibits a fingerprint texture under the POM, typical of a Ch\* phase. The distance between the stripes in the optical texture corresponds to the helical half-pitch ( $P/2$ ) of the Ch\*LC.

### **Preparation of SmA electrolyte solution**

A mixture of 8OCB/6CB (= 2/1 by weight), which exhibited a stable SmA focal conic fan-shaped texture or polygonal texture under the POM at room temperature, was prepared prior to the preparation of SmALC. Although 8OCB exhibits the SmA phase between 54.5 and 67 °C, a mixed LC system of 6CB and 8OCB was employed for the SmALC electrolyte solution, in order to achieve depression of the viscosity and tuning of the LC temperature range for electropolymerisation under magnetic field at room temperature. The SmALC electrolyte solution was prepared by dissolving TBAP (0.1 mg) and *ter*EDOT (monomer, 5 mg) in the 8OCB/6CB mixture (2/1, w/w, matrix LC, 0.5 g) under argon flow.

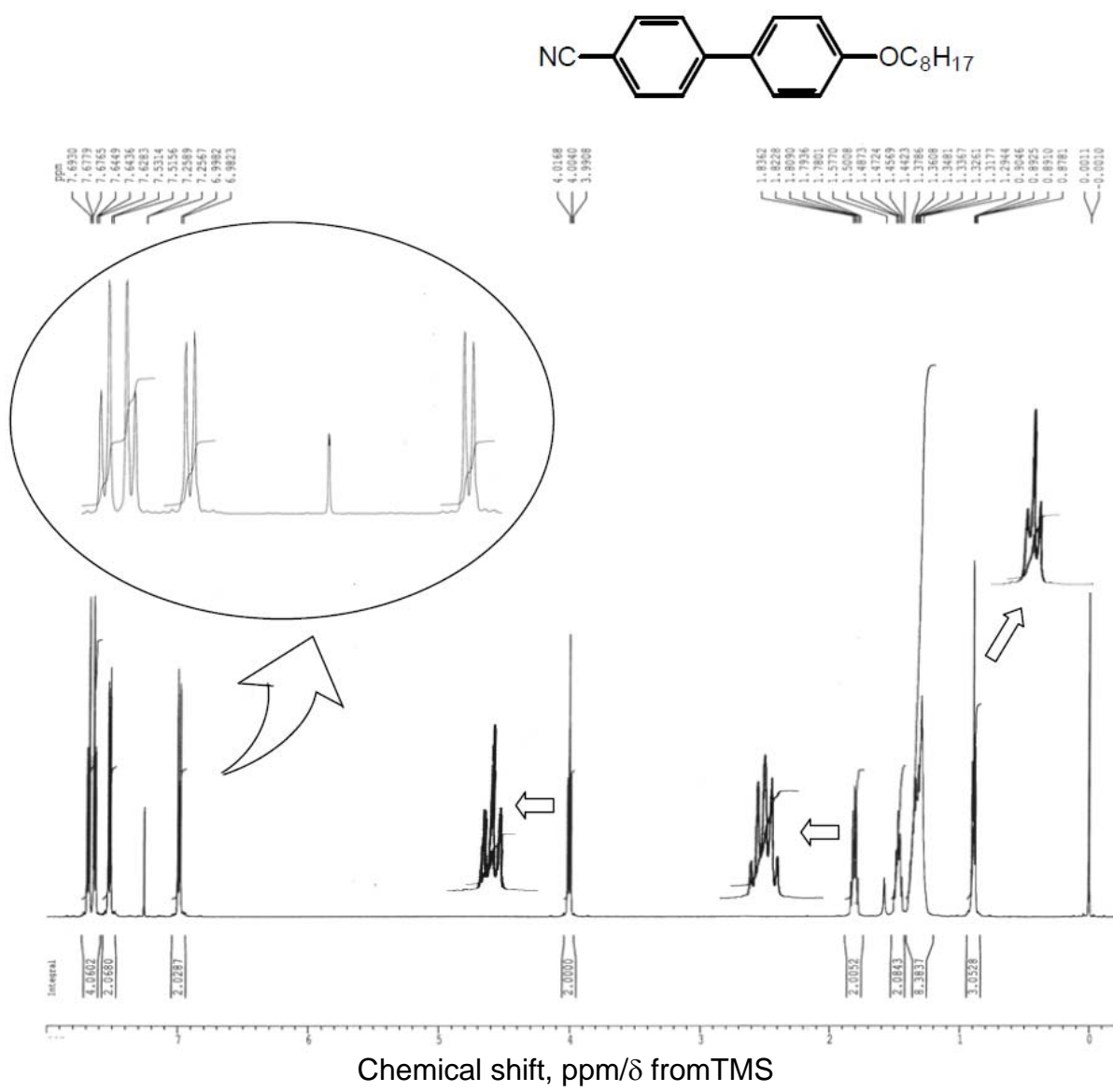


**Fig. S17.**  $^1\text{H}$  NMR spectrum of 8OCB in  $\text{CDCl}_3$ .

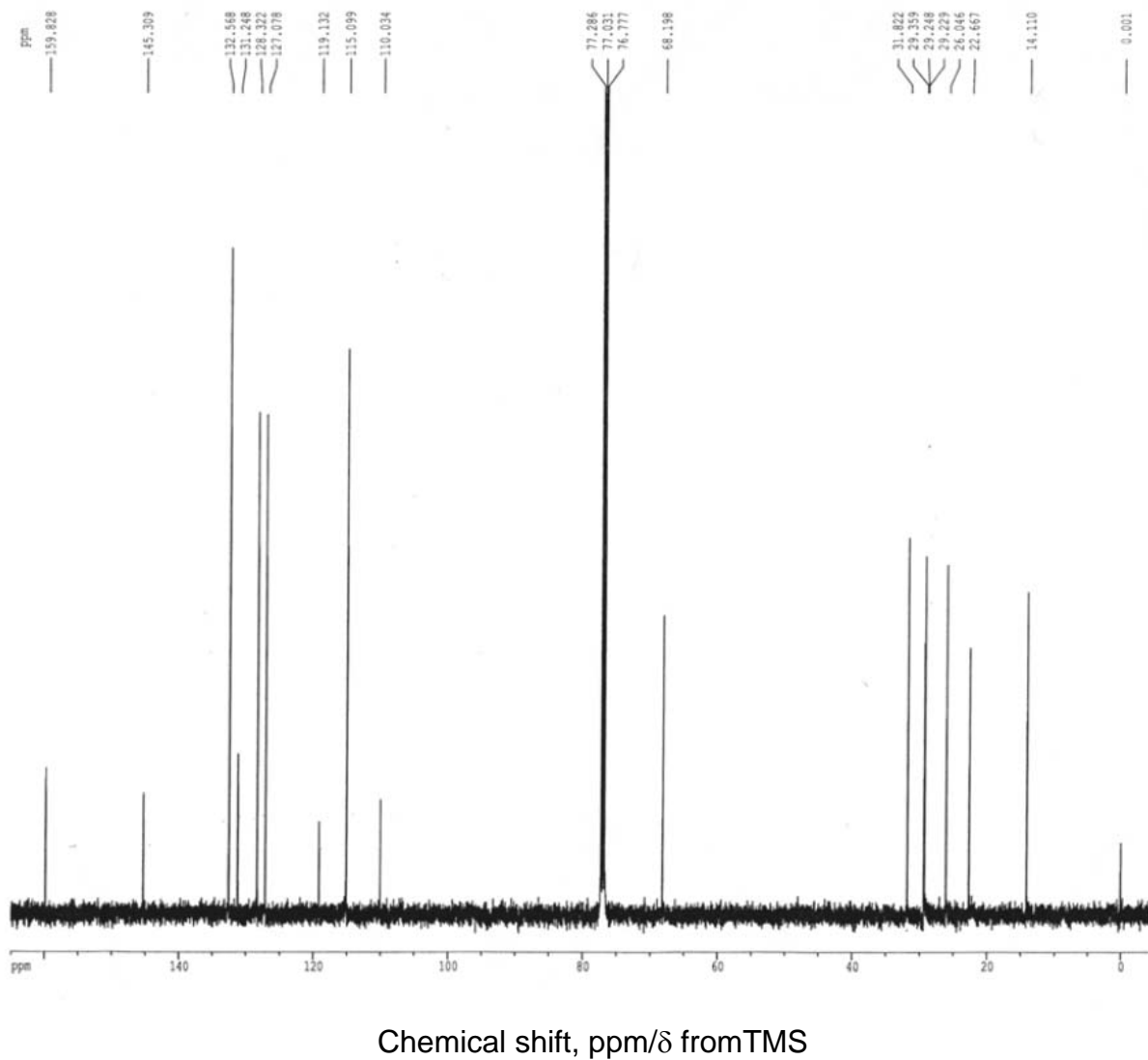
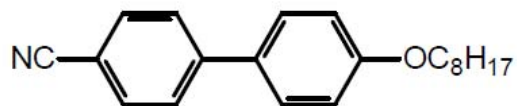


**Fig. S18.**  $^{13}\text{C}$  NMR spectrum of 8OCB in  $\text{CDCl}_3$ .